The ABC transporter DerAB of *Lactobacillus casei* mediates resistance against insect-derived defensins

Ainhoa Revilla-Guarinos [1,#], Qian Zhang [1], Christoph Loderer[1], Cristina Alcántara [2], Ariane Müller[3], Mohammad Rahnamaeian[4], Andreas Vilcinskas[4,5], Susanne Gebhard[6], Manuel Zúñiga [2] and Thorsten Mascher [1,#]

[1] Institut für Mikrobiologie, Technische Universität Dresden, Dresden, Germany

[2] Instituto de Agroquímica y Tecnología de Alimentos (IATA-CSIC), Valencia, Spain

[3] Institut für Zoologie, Technische Universität Dresden, Dresden, Germany

[4] Fraunhofer Institute for Molecular Biology and Applied Ecology, Department of Bioresources, Giessen, Germany

[5] Institute for Insect Biotechnology, Justus Liebig University Giessen, Giessen, Germany

[6] Department of Biology and Biochemistry, Milner Centre for Evolution, University of Bath, United Kingdom

RUNNING TITLE: **Defensin resistance in *Lactobacillus casei***

[#]Address correspondence to Ainhoa Revilla-Guarinos, ainhoa.revilla-guarinos@tu-dresden.de; or to Thorsten Mascher, thorsten.mascher@tu-dresden.de.

KEY WORDS: cell envelope stress response, antimicrobial peptide resistance, ABC transporter, two-component system, defensins, nisin

ABSTRACT

Bce-like systems mediate resistance against antimicrobial peptides in Firmicutes bacteria. *Lactobacillus casei* BL23 encodes an 'orphan' ABC transporter that, based on homology to BceAB-like systems, was proposed to contribute to antimicrobial peptide resistance. A mutant lacking the permease subunit was tested for sensitivity against a collection of peptides derived from bacteria, fungi, insects and humans. Our results show that the transporter specifically conferred resistance against insect-derived cysteine-stabilized αβ-defensins, and it was therefore renamed DerAB for *defensin resistance* ABC transporter. Surprisingly, cells lacking DerAB showed a marked increase in resistance against the lantibiotic nisin. This could be explained by significantly increased expression of the antimicrobial peptide resistance determinants regulated by the Bce-like systems PsdRSAB (formerly Module 09) and ApsRSAB (formerly Module 12). Bacterial two hybrid studies in *E. coli* showed that DerB could interact with proteins of the sensory complex in the Psd resistance system. We therefore propose that interaction of DerAB with this complex in the cell creates signaling interference and reduces the cell's potential to mount an effective nisin resistance response. In the absence of DerB, this negative interference is relieved, leading to the observed hyper-activation of the Psd-module and thus increased resistance to nisin. Our results unravel the function of a previously uncharacterized Bce-like orphan resistance transporter with pleiotropic biological effects on the cell.

IMPORTANCE

Antimicrobial peptides (AMPs) play an important role in suppressing the growth of microorganisms. They can be produced by bacteria themselves – to inhibit competitors – but are also widely distributed in higher eukaryotes, including insects and mammals, where they form an important component of innate immunity. In low GC Gram-positive bacteria, BceAB-like

47 transporters play a crucial role in AMP resistance but have so far been primarily associated with
48 inter-bacterial competition. Here, we show that the orphan transporter DerAB from the lactic acid
49 bacterium *Lactobacillus casei* is crucial for high-level resistance against insect-derived AMPs. It
50 therefore represents an important mechanism for inter-kingdom defense. Furthermore, our
51 results support a signaling interference from DerAB on PsdRSAB module that might prevent the
52 activation of a full nisin response. The Bce modules from *L. casei* BL23 illustrate a biological
53 paradox where the intrinsic nisin detoxification potential only arises in the absence of a defensin
54 specific ABC transporter.

55

INTRODUCTION

Antimicrobial peptides (AMPs) are found in all domains of life and constitute an important aspect of the natural immune response of many organisms (1, 2). AMPs are considered as an alternative to classical antibiotics, since the development of resistance has occurred to a lesser extent (3, 4). One prominent mechanism of action of AMPs is binding to lipid II, leading to the inhibition of bacterial cell wall biosynthesis, often followed by pore formation with the concomitant release of cell metabolites and the loss of membrane potential (5-7). Most AMPs are structurally very diverse, amphipathic molecules composed of 5-60 amino acids with a net positive charge (http://aps.unmc.edu/AP/main.php (8)). Nisin and subtilin are elongated and flexible, positively charged type A lantibiotics, while mersacidin is a more globular and rigid type B lantibiotic with net negative charge (9). Insect AMPs such as cecropins have an α-helical structure, while defensins have a cysteine-stabilized structure consisting of an N-terminal loop followed by an α-helix and an antiparallel β-sheet (CSαβ), which are linked by disulfide bridges (10, 11).

Since AMPs represent common threats in microbial habitats, bacteria have developed a wide range of different AMP resistance mechanisms (3, 12). General or non-specific resistance is conferred by changing the bacterial surface properties. The *dlt* (D-alanyl-lipoteichoic acid) operon mediates the D-alanylation of lipoteichoic and wall teichoic acids (13, 14), while expression of *mprF* ("multiple peptide resistance factor") modifies anionic phospholipids of the membrane with L-lysine or L-alanine (15, 16). In both cases, the resulting decrease in the net negative charge of the bacterial envelope reduces the access of cationic AMPs to their surface targets, thereby conferring resistance. In contrast to this general AMP resistance, ABC transporters constitute compound-specific resistance determinants for AMP detoxification by actively removing the peptides from their site of action (17).

Bce-like systems, named after BceAB from *Bacillus subtilis*, represent a unique type of AMP-detoxifying ABC transporters (18, 19). They most likely consist of two nucleotide-binding domain (NBDs) subunits (ATPases) and a membrane spanning domain (MSD) subunit (permease) (20) and are functionally and genetically associated with BceRS-like two-component systems (TCS) (21, 22). The transporter confers resistance by a target-protection mechanism, where constant removal of the AMP from its cellular target keeps sufficient amounts of lipid II cycle intermediates available to ensure continued cell wall synthesis (23, 24). The transporter works in a sensory complex with the histidine kinase (HK), BceS (20). Signaling within this complex is activated in response to transport activity (25), which is achieved by the transporter directly controlling the conformational state of the HK (26). Upon activation, BceS then phosphorylates BceR, its cognate response regulator (RR), which in turn induces the expression of *bceAB* and sometimes additional target genes, which ensures antibiotic resistance. Since this detoxification process also removes the antibiotic from its site of detection (i.e., the transport activity of the resistance transporter decreases), Bce-dependent signalling is gradually switched off again (25, 26).

So-called 'dual function' BceAB-like transporters are required both for sensing the presence of the AMPs (input) and their detoxification (output). However, a division of labor between Bce-like transporters can be found in some systems: here, a specialized 'sensing transporter' perceives the signal and passes this information on to its cognate TCS, which in turn leads to the expression of a second 'resistance transporter' that removes the AMP from the cell surface (12, 27).

So far, the specificity of BceAB-like transporters could not be correlated with any particular characteristic feature of the AMPs, such as structure, origin, modification or mechanism of action (17, 21, 28). Some transporters can confer resistance against structurally very different AMPs, while at the same time being able to distinguish between very similar compounds. For example, the Psd system of *B. subtilis* responds to actagardine and enduracidin but not to mersacidin or

ramoplanin (29). Intriguingly, BceAB-like transporters can even be induced by AMPs against which they do not mediate any resistance: e.g. PsdAB is induced by actagardine but does not confer resistance against it (29). This behaviour indicates that sensing and removal of AMPs are two separable functions of BceAB-like transporters, an assumption that has been genetically verified for BceAB of *B. subtilis* (30).

L. casei BL23 encodes 17 TCSs (31), two of which, TCS09 and TCS12, are homologous to BceRS from *B. subtilis.* Both systems are genomically and functionally associated with BceAB-like transporters, ABC09 and ABC12 respectively, and constitute functional Bce-like units that were initially referred to as Module 09 and Module 12 (32). Module 09 is a stand-alone detoxification system, in which ABC09 is a dual function transporter and *abc09* is the only known target operon of RR09. TCS09 responds to nisin via ABC09 and induces the expression of the transporter, which then confers nisin resistance (Fig. 1). Module 09 additionally confers resistance against bacitracin, plectasin and subtilin (32). Because its inducer/substrate spectrum and regulatory behaviour resembles that of PsdRSAB from *B. subtilis* (29), we renamed Module 09 to PsdRSAB, for *peptide antibiotic sensing and detoxification.* For Module 12, ABC12 is a sensing transporter that is not involved in the detoxification process. In response to nisin, the cognate RR12 instead induces the expression of a larger regulon that includes the *dlt* operon, the *mprF* gene and an operon encoding an orphan BceAB-like ABC transporter of unknown function (Fig. 1). Module 12 deletion mutants are sensitive to bacitracin, nisin, subtilin, mersacidin, plectasin and vancomycin, mainly due to the impaired functionality of the Dlt system, which also renders these mutants acid sensitive (33). This organisation and behaviour is similar to the Aps system of *Staphylococcus epidermidis*, which regulates the expression of the *dlt* operon, the *mprF* gene and the *vraFG* ABC transporter in response to AMPs (34). We therefore renamed Module 12 to ApsRSAB standing for *antimicrobial peptide sensor.*

In this report, we investigated the function of the ApsR-dependent orphan ABC transporter from *L. casei* BL23 in response to AMPs. A mutational study demonstrated that the orphan transporter is a *defensin*-specific *resistance* transporter, which we therefore renamed DerAB, with DerA (locus *LCABL_21680*) forming the NBD (ATPase) and DerB (locus *LCABL_21670*) the MSD (permease) subunits of the system. Absence of a functional DerAB transporter not only increased the sensitivity to defensins, but remarkably also resulted in a decreased sensitivity to nisin. This surprising finding could be explained by gene expression studies in *ΔderB* mutant showing hyper-activation of the Psd and Aps regulated systems in response to nisin. Moreover, bacterial two-hybrid assays showed that DerB can interact with PsdS and PsdA. Based on these results, we propose that non-productive protein-protein interactions of DerAB with the PsdRSAB sensory complex might result in regulatory interference within Psd-module signal transduction that modulates the induction of the nisin resistance response.

RESULTS

DerAB mediates resistance against insect-derived defensins but renders L. casei nisin sensitive

ApsRSAB from *L. casei* BL23 is involved in resistance against several bacteriocins and the fungal peptide plectasin, and it controls the expression of the BceAB-like orphan transporter DerAB (32), which has so far not been studied with respect to its physiological role. Since all known BceAB-like transporters mediate AMP resistance (17), we tested the sensitivity of a *ΔderB* strain against a wide range of different AMPs. No differences in MIC values were obtained for bacitracin, mersacidin and vancomycin when comparing the *ΔderB* strain with the parental strain BL23 (Table 1). While the absolute MIC values for plectasin (> 40 µg ml^{-1}) and subtilin (3% (v/v)) were also identical, the *derB* mutant showed slightly reduced growth in the presence of these peptides compared to the wild type (Fig. 2A and B, respectively). Surprisingly, the *ΔderB* strain was

ten-fold more resistant against nisin than the parental strain (Fig. 2C). Since nisin and subtilin are structurally similar type A lantibiotics, these results were puzzling. We had previously shown that PsdAB from BL23 is involved in nisin and subtilin resistance (32), therefore we reasoned that a contribution to resistance/sensitivity mediated by DerAB should be revealed in a double mutant *ΔderBΔpsdB.* For subtilin, we did not observe any significant contribution of DerAB to mediating resistance (the MIC of subtilin was 0.5% (v/v) for both *ΔpsdB* and *ΔderBΔpsdB*). In contrast, the MIC of nisin was 0.5 µg ml^{-1} for BL23, 0.3 µg ml^{-1} for the more sensitive *ΔpsdB* and 5 µg ml^{-1} for the highly resistant strain *ΔderB,* while the *ΔderBΔpsdB* mutant had an intermediate phenotype with an MIC of 1 µg ml^{-1}, being this double mutant more resistant to nisin than the wild type. These results demonstrate that a *derB* deletion could rescue the nisin sensitivity of a *psdB* mutant and corroborated the relevance of DerAB in the induction of a full nisin resistance response. A more detailed investigation of the nisin resistance phenotype of *ΔderB* strain is described below.

Since *L. casei* strains can be found in the human gastrointestinal tract (35), where it is exposed to AMPs of the innate immune defence (36), we next tested the sensitivity of the strains to human AMPs. LL37 is a human cathelicidin (37) that functions as a specific activator of the Bce-like ApeRSAB (formerly YxdJKLM) module of *B. subtilis* (38, 39), while hBD1 is a human defensin that is activated by reduction of its disulfide bridges (40, 41). We did not observe any differences in sensitivity to LL-37 or hBD1 between BL23 and *ΔderB* strains (Table 1). In contrast, strains carrying *ΔapsR, ΔapsB* and *ΔdltA* mutations were more sensitive to LL-37 than the BL23 wild type (Fig. S1), indicating a role of ApsRSAB in resistance against LL-37, likely by regulating the activity of the Dlt system.

Lactobacilli can also be found in the microbiota of insects (42, 43). Next, we tested the sensitivity of BL23 and *ΔderB* strains against a collection of 18 insect-derived AMPs. Both strains were resistant against even the highest concentrations of most insect AMPs tested (Table 1).

However, for three defensins we could observe significant differences in resistance. The *ΔderB* mutant was slightly more sensitive to LSer-Def4 (BR090, Fig. 2D) and much more sensitive to sapecin A (BR080; MIC > 160 µg ml^{-1} for BL23, 80 µg ml^{-1} for *ΔderB*) and Lser-Def3 (BR092; MIC > 320 µg ml^{-1} for BL23, 320 µg ml^{-1} for *ΔderB*) (Figs. 2E and F, respectively) than the parental strain, indicating that DerAB mediates resistance against these compounds. To confirm that the observed phenotype was specific to and directly caused by the loss of DerAB, we repeated the sensitivity experiment for sapecin A on a strain carrying an ectopic copy of *derB* to complement the *ΔderB* mutation. Indeed, complementation restored much of the original resistance (Fig. S2). The slight remaining differences to the wild type are likely due to altered expression levels of *derB* between the native and ectopic copy, as was observed for complementation of a *bceB* mutant of *B. subtilis* (44). Taken together, the data indicate that DerAB specifically mediates resistance against insect-derived AMPs.

Subsequent microscopic studies revealed significantly different morphological aberrations in the *ΔderB* strain when challenged with different AMPs (Fig. 3 and Sup. Table 1). No morphological differences were found between BL23 and *ΔderB* strains after exposure to BR005 (Fig. 3C and D), BR081, BR087, BR088, BR091 or subtilin 2% (v/v) (data not shown). In contrast, the *ΔderB* strain was strongly affected after exposure to 400 µg ml^{-1} BR090, showing chaining (Fig. 3J and K), aberrant morphologies and cells becoming phase transparent (Fig. 3F). Although minor changes were also observed in the wild type treated with BR090, these were far less pronounced (Fig. 3E). After incubation with BR080 (Fig. 3G and H) or BR092 (data not shown), the chaining phenotype of *derB* deletion mutant was even more pronounced (Fig. 3J and K), whilst the parental strain remained unaffected. These morphological changes of the *ΔderB* strain after exposition to BR080, BR090 and BR092 are in good agreement with the sensitivity phenotypes observed for these AMPs (Fig. 2).

198 *L. casei* mutants in *apsRSAB* are defective in D-alanylation of teichoic acids, resulting in a
199 more negative surface charge and a higher AMP sensitivity of *ΔapsR*, *ΔapsB* and *Δdlt* compared to
200 the parental strain (32). A possible explanation for the observed sensitivity of the *ΔderB* strain
201 could therefore be that DerAB somehow contributes to the regulation of the Dlt system through
202 ApsRS. However, measurements of the cell surface charge by cytochrome *c* binding assays (32, 45)
203 did not show any significant differences between BL23 and *ΔderB* strain (Fig. S3), thereby ruling
204 out this cause for the higher AMP sensitivity of the *derB* mutant.

205 Since the *ΔderB* strain showed the strongest sensitivity phenotypes when exposed to insect-
206 derived defensins (Fig. 2E and F), we additionally investigated the contribution of DerAB to
207 resistance against crude extracts derived from larvae of the dipteran species black soldier fly
208 *Hermetia illucens* (see Materials and Methods for their preparation), which are particularly prolific
209 sources of broad-spectrum antimicrobial substances (46). A recent transcriptome study identified
210 53 genes encoding putative AMPs from different families, half of which are putative defensins
211 (47). Amongst those, the defensin-like peptide 2 (DLP2;
212 ATCDLLSPFKVGHAACALHCIAMGRRGGWCDGRAVCNCRR) and the defensin-like peptide 4 (DLP4;
213 ATCDLLSPFKVGHAACAAHCIARGKRGGWCDKRAVCNCRK) have been characterized (48, 49). Both
214 defensins possess a CSαβ structure and are active against Gram-positive bacteria. If DerAB is a
215 defensin-specific resistance transporter, its absence should render *L. casei* also sensitive to
216 *H. illucens* extracts. Indeed, the *ΔderB* strain was over 100-fold more sensitive than the parental
217 strain (Fig. 2G; MIC is 5 % (v/v) for BL23 and 0.04 % (v/v) for *ΔderB*), thereby confirming its role in
218 conferring resistance against AMPs produced by *H. illucens*. Besides the strong effect on
219 resistance, we observed some morphological differences in the form of elongated and chaining
220 cells in the *ΔderB* strain after exposition to *Hermetia* larvae extracts (Fig. S4).

ApsRSAB regulates different layers of resistance against antibiotics produced by H. illucens larvae

The AMP resistance determinants of *L. casei* are controlled by the Psd and Aps modules: the PsdRSAB system regulates the target operon *psdAB*, and the ApsRSAB system regulates the expression of the *dlt* operon, *mprF* gene and *derAB* transporter (32) (Fig. 1). Because of the potency of the *H. illucens* larval extracts and the strong difference in sensitivity between the *derB* deletion mutant and the parental strain, we next aimed at analysing the hierarchy within the AMP resistance network orchestrated by the Psd and Aps modules and the individual contributions of their target genes to protecting *L. casei* against the combined challenge of *H. illucens* extracts. Towards this goal, we performed a comprehensive mutational study of the individual components of the AMP resistance network of *L. casei* (Fig. 4).

The MIC values for strains *ΔpsdR* and *ΔpsdB* were similar to that of the wild type strain BL23 (5% (v/v)), indicating that the stand-alone Psd module is not involved in mediating resistance against larval extracts (Fig. 4). In contrast, both mutants that rendered the Aps system dysfunctional, *ΔapsR* and *ΔapsB* strains, were highly sensitive to *H. illucens* extracts, with an MIC of 0.01% (v/v) (500-fold more sensitive than the wild type).

Next, we determined the MIC for all three Aps-dependent AMP resistance determinants deleted individually. While both the *ΔmprF* and *ΔdltA* mutants showed a slight increase in sensitivity compared to the wild type, the most marked effect was again observed in the *ΔderB* strain (Fig. 4). These data clearly show that the DerAB transporter, provides the primary resistance layer against the AMPs present in the larval extract, while D-alanylation of teichoic acids and – to a smaller extent – the L-lysinylation of phospholipids represent a secondary layer of resistance. In agreement with this hierarchy, the MIC of a *ΔderBΔdltA* double mutant (0.02% (v/v)) was further increased compared to the single mutants, that is, 16-fold more sensitive than *ΔdltA* strain and 2-

fold more sensitive than *ΔderB* strain. To rule out any minor contributions to resistance by the Psd system, we also tested a *ΔderBΔpsdB* double mutant, but could not detect any changes relative to the *ΔderB* single mutant. Taken together, our results demonstrate that a clear hierarchical organization of multiple layers ensure protection of *L. casei* against insect-derived AMPs, and all resistance determinants relevant for counteracting the AMPs contained in *H. illucens* extract are under control of a single module: ApsRSAB.

Resistance determinant genes are transcriptionally over-expressed in ΔderB strain in response to nisin.

As mentioned above, the *ΔderB* strain unexpectedly showed a ten-fold increase in resistance against nisin (MIC 5 μg ml^{-1}; MIC for parental strain 0.5 μg ml^{-1}) (Table 1 and Fig. 2C). PsdAB is involved in nisin resistance and partially contributes to the hyper-resistance of *ΔderB* (MIC value for double mutant *ΔderBΔpsdB* of 1 μg ml^{-1}). However, the main nisin resistance determinant of *L. casei* is the Dlt system, since the *ΔdltA* mutant was 12.5-fold more sensitive to nisin than the wild type (MIC for *ΔdltA* strain is 0.04 μg ml^{-1}) (32). We have previously shown that transcription of the *psdAB* and *dltA* genes is induced in a nisin-dependent manner in BL23, as are the genes *derAB* and *mprF* (32). We therefore hypothesized that the increased resistance of *ΔderB* strain might be due to a higher expression level of the nisin resistance determinants in this mutant. Thus, we tested the response of these genes following nisin exposure in the *ΔderB* strain background compared to the wild type, following the previously established procedure (32).

Expression of *psdR*, *apsB*, *apsA* and *apsR* was not induced by nisin in either strains (Fig. 5A), in agreement with the role of PsdRS and ApsRSAB in signaling rather than resistance (32). Strikingly, nisin exposure of the *ΔderB* strain led to a notable increase of induction of nisin resistance genes compared to the BL23 wild type (Fig. 5A): the genes encoding the transporters (*psdA*, *psdB* and *derA*) were up to ten-fold stronger induced in the *ΔderB* strain than in the wild

type. Likewise, *dltA* and *mprF* also responded more strongly (~ 2.5-fold and ~ 3.5-fold, respectively) in the mutant. Importantly, no significant differences in gene expression were found between *ΔderB* and the parental strain in reference conditions (Fig. S5), showing that the increased induction was due to a hyper-response to nisin exposure and not general changes in gene expression upon *derB* deletion. Moreover, since the systems involved in nisin resistance in *L. casei* BL23 also mediate subtilin resistance (32), we next tested the response of these genes following subtilin exposure in the *ΔderB* strain background compared to the wild type. Noticeably, no significant differences in gene expression were found between *ΔderB* and the parental strain in response to subtilin (Fig. 5B and Fig. S5). We therefore concluded that the increased nisin resistance of *ΔderB* strain was due to an over-expression, compared to the parental strain, of the nisin resistance determinants *psdAB*, *mprF* and the *dlt* operon, and that this response was specific for nisin.

DerAB may interfere with signaling through spurious protein-protein interactions.

We next investigated the molecular basis for the observed hyper-induction of nisin resistance genes in the *ΔderB* strain. For the BceRSAB system of *B. subtilis*, it is known that signaling depends on a sensory complex formed between the transport permease BceB and the histidine kinase BceS (20). Moreover, signaling requires a functional transporter that is capable of ATP hydrolysis (25, 44), i.e. correct interaction between the permease BceB and the ATPase (BceA) subunits. Since it could be possible that DerAB may somehow interfere with one or more of the nisin-responsive signaling pathways in the cell, we performed bacterial two-hybrid experiments of all involved protein partners to test if the permease DerB is able to interact with any of the components of the Psd or Aps resistance systems (Fig. 6 and Fig. S6). In addition to the expected interaction between DerB and DerA, we also obtained positive results for DerB paired with PsdA (Fig. 6). It is possible that such non-cognate binding of the ATPase PsdA by DerB may reduce the ability of the PsdAB

transporter to trigger signaling via PsdS. Moreover, we observed clear interactions between DerB and PsdS (Fig. 6). It is likely that such non-cognate interactions between the permease DerB and the Psd histidine kinase would interfere with native signaling. Relief of this interference in the *ΔderB* strain could then explain the observed increase in the amplitude of the nisin response and resulting nisin resistance.

Unfortunately, similar bacterial two-hybrid experiments with the Aps proteins were less conclusive because several of the fusion constructs did not even give positive results with their known interaction partners (Fig. S6); consequently, these assays were not informative for potential interactions between DerAB and the Aps system.

DISCUSSION

ABC transporters acting as detoxification mechanisms are of major importance as AMP resistance systems in Firmicutes (17). In this study, we unraveled the function of DerAB in *L. casei* BL23, which belongs to the BceAB-like group of transporters.

Our results demonstrate that from the available panel of antimicrobial compounds, four CSαβ defensins (plectasin, sapecin A, LSer-Def4 and LSer-Def3) are the most relevant substrates of DerAB. Such defensins are ubiquitously produced in plants, insects, mussels and fungi and form an important component of the innate immunity (10). In addition to defined compounds, we also demonstrated the relevance of DerAB for the survival of *L. casei* when challenged with a potent mix of insect AMPs from *H. illucens* larvae. Lactobacilli grow in a variety of nutrient-rich carbohydrate-containing habitats. In addition to its well-known roles in fermentation and spoilage of food, *L. casei* is also found in the oral cavity, gastrointestinal and genital tracts of humans and other animals (50). Moreover, different *Lactobacillus* species have been found in the microbiota of insects (42, 43). It is usually assumed that lactobacilli present in food come from the food

316 processing equipment, raw foodstuffs such as plant material or faecal contamination, but it may
317 appear that insects may play a role in the dissemination of *L. casei*. A recent study has provided
318 evidence suggesting that insects are the natural reservoir of *Lactobacillus sanfranciscensis*, an
319 organism involved in sourdough fermentation (51). Interestingly, in this study, Operational
320 Taxonomic Units (OTUs) belonging to *L. casei* group were the second most numerous after
321 *L. sanfranciscensis* within lactobacilli OTUs (51). Our results suggest that possession of DerAB may
322 protect *L. casei* in different AMP-enriched environments of eukaryotic origin, including insects,
323 and thereby enable it to colonise its hosts.
324 Furthermore, by testing the sensitivity of our collection of mutants to extracts from
325 *H. illucens* larvae, which contain a very potent mixture of AMPs (46, 47), we showed that BL23
326 possesses several layers of AMP resistance. In this network, DerAB is the defensin-specific primary
327 resistance mechanism, while the Dlt system and MprF protein constitute the secondary, more
328 general resistance layer by altering the bacterial surface charge (Fig. 1). Remarkably, in
329 *Bacillus subtilis,* the response to bacitracin also consists of a hierarchy of different layers of
330 resistance: the BceAB transporter constitutes the primary (drug-sensing and highly efficient)
331 resistance determinant, and the LiaIH system together with the BcrC phosphatase constitute the
332 secondary (damage-sensing and less efficient) layer of resistance (52). Thus, a clear hierarchical
333 organization of multiple layers ensure protection of both *L. casei* and *B. subtilis* against AMPs.
334 Interestingly, not only the individual components of the resistance networks are different between
335 *L. casei* (DerAB transporter, Dlt operon and MprF protein) and *B. subtilis* (BceAB transporter, LiaIH
336 system and BcrC phosphatase) (52), also, the resistance layers are controlled by separate cell
337 envelope stress systems in *B. subtilis* (52), whereas all resistance determinants relevant for
338 counteracting the AMPs contained in *H. illucens* extract are under control of a single module,
339 ApsRSAB, in *L. casei*.

So far, the substrate specificity of BceAB-like transporters could not be related with any particular feature of the respective AMPs (17, 21, 28). Our results for DerAB indicated a preference for CSαβ defensins, e.g. plectasin, sapecin A (BR080), LSer-Def4 (BR090) and LSer-Def3 (BR092). Surprisingly, DerAB does not confer resistance against the structurally closely related defensins lucifensin (BR088), BR081, BR087, LSer-Def7 (BR089) and LSer-Def6 (BR091) (Table 1). This indicates that DerAB can distinguish between very similar CSαβ defensin substrates, a situation reminiscent of the results obtained for the Psd module of *B. subtilis* (29). We performed a structural analysis of all tested candidates mentioned above to further investigate this apparent specificity of DerAB for some defensins (Fig. 7). The investigated defensins show a moderate sequence conservation with an average sequence identity of 50 % (Fig. S7). The overall structure of the defensins is well conserved with all available structures harboring a cysteine-stabilized α-helix β-sheet (CSαβ) motif. The main structural deviations are in the N-terminal loop region, which is also least well conserved, both with respect to its size and amino acid sequence (Fig. 7). No obvious pattern of structural determinants distinguishing substrates from non-substrates could be extracted, in line with previous studies on the substrate specificity of BceAB-like transporters (21).

The most puzzling result that we obtained during our initial sensitivity screen was the hyper-resistance of the *derB* deletion mutant against the lantibiotic nisin. Transcriptional studies in the *ΔderB* strain in response to nisin demonstrated that the absence of this transporter resulted in an over-induction of *mprF*, the *dlt* operon and *psdAB*. Both the Dlt system and the PsdAB transporter are crucial for nisin resistance in *L. casei* (32). Our results strongly suggest that their over-expression accounts for the hyper-resistance of the *ΔderB* strain to nisin. This hypothesis is supported by independent studies in other Firmicutes bacteria that demonstrated the role of *dlt* expression levels for AMP resistance. Acquisition of nisin resistance in *Lactococcus lactis* IL1403 was partly due to higher expression levels of the *dlt* operon (53). Similarly, strains of

364 *Staphylococcus aureus* Sa113 bearing additional copies of the *dlt* operon showed an increased
365 level of D-alanine in LTA and WTA, which led to an increased nisin resistance (45).

366 In the case of the *ΔderB* strain investigated here, increased nisin resistance could, however,
367 not be explained by acquisition of additional copies of resistance genes. Instead, we could show
368 that DerB has the ability to interact with components of the Psd resistance system. We propose
369 that such spurious interactions with non-cognate protein partners likely have a negative impact on
370 signal transduction. That is, in the presence of nisin, not all PsdS histidine kinases receive a signal
371 from their cognate transporter PsdAB, because a proportion is in a non-productive complex with
372 DerB. This interference is removed upon *derB* deletion, allowing the full potential activation of
373 *psdAB* expression and thus a greater level of resistance against the AMP. Of note, whereas the
374 strain C-*derB,* carrying an ectopic copy of *derB* in the *derB* deletion mutant background,
375 complemented sensitivity to the defensin sapecin A, the restoration of nisin sensitivity was only
376 very weak (Fig. S2). Likely the ectopic copy of *derB* did not result in the same protein levels of DerB
377 in the cell and therefore the interference with normal Psd signaling was not observed. However,
378 indirect evidence supporting this interference model is available. Results of gene expression
379 previously reported (32) for mutants defective in the ApsRSAB system, and results reported here
380 for *ΔderB* (Fig. 5A and Fig. S5), showed an increase in expression of *psdAB* in the presence of nisin,
381 suggesting that a decrease in the ratio of DerAB over PsdAB results in increased PsdRSAB signal
382 transduction. Furthermore, results obtained with subtilin (Fig. 5B and Fig. S5) show that this is a
383 nisin-specific effect. To our knowledge, such a negative effect of one Bce-like resistance system on
384 the function of another has not been previously reported. Also, why this phenotype is observed
385 with nisin and not with a closely related lantibiotic such as subtilin, is still unclear.

386 We previously showed that Bce-like systems are wide-spread among Firmicutes bacteria,
387 and that many species contain multiple copies with different substrate specificities (21). Often, the

388 closest homolog to a given system is found in a different species, while the paralogs within a single
389 species can be quite distantly related (21). For the Bce-like systems characterized to date, signaling
390 between transporter and two-component system appears to be highly specific and no accidental
391 cross-talk has been reported. The example of DerAB reported here may constitute an interesting
392 evolutionary intermediate where the interaction specificity is not yet completely insulated,
393 allowing non-productive interference with the Psd system. In this scenario, in the presence of
394 nisin, the interference by DerAB should pose a significant fitness burden on the cell. However, we
395 did not observe any effects of a *derB* deletion on gene expression when cells were grown in un-
396 challenged reference conditions or after subtilin exposure (Fig. 5B and S5), suggesting that DerAB
397 has no negative effect in most situations. An alternative scenario could then be that the
398 interference by DerAB is in fact beneficial to prevent an over-reaction to nisin that could also pose
399 a fitness burden to the cell. Interestingly, a similar hidden potential in the response to nisin
400 mediated by Bce-like systems was also previously reported in *S. aureus* (54). While beyond the
401 scope of the present study, it would be interesting to investigate if, under suitable experimental
402 pressure, *L. casei* BL23 could evolve increased signaling specificity and circumvent the interference
403 from DerAB.

404 In summary, in this work we demonstrated that DerAB is a defensin-specific resistance
405 transporter that constitutes a primary layer of the *L. casei* cell envelope stress response. Its
406 expression is controlled by the Aps module that also regulates the secondary, more general, layers
407 of resistance, the Dlt system and MprF. Given the high degree of protection against insect-derived
408 AMPs, it appears likely that the physiological role of DerAB is in host-microbe interactions and may
409 allow *L. casei* to avoid innate immune defenses to colonise its eukaryotic hosts.

410 **EXPERIMENTAL PROCEDURES:**

411 ***Bacterial strains, plasmids and grown conditions***

412 Table 2 and 3 list the strains and plasmids, respectively, used in this study. *Escherichia coli*
413 DH10β and *Lactococcus lactis* MG1363 were used as intermediate hosts for cloning purposes.
414 *E. coli* strains were grown in LB medium at 37°C with aeration. *L. lactis* strains were grown in M17
415 medium supplemented with 0.5 % (w/v) glucose at 30°C under static conditions. *L. casei* strains
416 were grown in MRS broth (Oxoid) at 37°C under static conditions. 1.5 % (w/v) agar was added to
417 prepare the corresponding solid media. Strains were stored at -80°C in their corresponding growth
418 media containing 20 % (v/v) glycerol. Ampicillin 100 µg ml^{-1} was added to *E. coli*, and erythromycin
419 5 µg ml^{-1} was added to *L. lactis* and *L. casei*, when required.

420 ***Construction of mutants***

421 Oligonucleotides used in this study are listed in Table 4. Cloning in *E. coli* was performed
422 following standard methods (55). *E. coli* strains were transformed by electroporation with a Gene
423 Pulser apparatus (Bio-Rad), as recommended by the manufacturer; *L. lactis* strains were
424 transformed by electroporation (56) and *L. casei* strains were transformed as described previously
425 (57).

426 For a complete deletion of gene LCABL_21670 (*ΔderB*) from *L. casei* BL23, two DNA
427 fragments of approximately 700 bp upstream and downstream of the target gene were amplified
428 from genomic DNA using primers pairs RG062-063 and RG064-065 (see Table 4). All subsequent
429 steps of mutant construction were performed as previously described (32). Strain C-*derB* with the
430 complementation of the *derB* deletion was achieved by cloning the corresponding gene and
431 potential ribosome binding site (12 pb intergenic region between *derA*-*derB*), with primer pair
432 RG220-221 (*SpeI* and *BglII* restriction sites; Table 4), under the constitutive P1 promoter in the
433 expression vector pT1NX (58). The resulting plasmid *pT1-RBS$_{derB}$derB* (Table 3) was used to
434 transform *L. lactis* MG1363, and transformants were checked by sequencing of the inserted

fragment. Subsequently, plasmid *pT1-RBS$_{derB}$derB* was used to transform *L. casei ΔderB*, resulting in strain *L. casei C-ΔderB* (Table 2) which was maintained with erythromycin selection.

Double mutant strains *ΔderBΔdltA* and *ΔderBΔpsdB* were obtained by insertional inactivation of genes LCABL_08550 (*dltA*) and LCABL_16400 (*psdB*), respectively, in *L. casei ΔderB* mutant background. A procedure similar to the previously described to obtain insertionally inactivated single mutants of genes LCABL_08550 and LCABL_16400 was followed (32).

Bacterial two-hybrid assays

We constructed C-terminal and N-terminal translational fusions of the T18 and T25 domains of the adenylate cyclase CyaA of *Bordetella pertussis* for each protein individually (40 constructs; Table 3), to test protein-protein interactions between DerAB and PsdRSAB module, and between DerAB and ApsRSAB module. Fusions were tested in pairwise combinations in *E. coli* BTH101 (59). For each co-transformation mixture, 3 times 10 µl were spotted onto LB agar plates containing 1 mM isopropyl-β-D-1-thio-galactopyranoside (IPTG) and 100 µg ml^{-1} 5-bromo-4-chloro-3-indolyl-β-D-galactopyranoside (X-Gal) with selection for ampicillin and kanamycin resistance. Plates were incubated at 30 °C for 48 h. Positive interaction results were identified by the formation of blue colonies.

Source or preparation of eukaryotic AMPs and subtilin

HBD-1 and LL-37 were purchased from Sigma-Aldrich™ (SRP3011 and 94261, respectively) and were reconstituted according to manufacturer instructions. The insect AMPs shown in Table 1 were selected according to their reported structural and functional properties, synthesized and purified to >95%. Cecropin 1 (from *Eristalis*) was synthesized by PepMic (Pepmic Suzhou, Jiangsu, China). Cecropin A (from *Hyalophora* and *Aedes*), Stomoxyn (from *Stomoxys*) and Sarcotoxin IA were synthesized by JPT (JPT Peptide Technologies GmbH, Berlin, Germany). The rest of the peptides were synthesized by Covalab (Covalab S.A.S., Villeurbanne, France), based on the

sequence of the mature peptides. All peptides were lyophilized for storage and were resuspended and diluted in double-distilled water. Excluding *Aedes* and *Eristalis* cecropins, all other cecropins and *Stomoxys* stomoxyn were modified by the C-terminal amidation.

Larvae of the black soldier fly (*Hermetia illucens*) were obtained from a pilot rearing plant in Grimma, Saxony, Germany, and grown at 24°C in the laboratory. *H. illucens* larvae were induced as previously described (39, 46) by injecting a fungal spore suspension (spores of *Verticillium lecanii* and *Metarhizium anisopliae*) into the haemolymph and by feeding a bacterial mix (*E. coli*, *Micrococcus luteus*, *Pseudomonas fluorescens*, *B. subtilis*) to simulate an infection and boost AMP production. The larvae were pricked as previously described (46). Aqueous larval extract from *H. illucens* was prepared as previously described (46) and was considered to be at a concentration of 100% (v/v) for the MIC assays.

B. subtilis ATCC 6633 was grown in medium A to induce subtilin production as in (60). Culture supernatant was collected and was considered to be at a concentration of 100% (v/v) for MIC assays.

Antibiotic sensitivity testing

MIC assays were performed in 96-well microtiter plates as previously described (32). Overnight cultures of the strains under study were prepared with antibiotic selection when required but, no antibiotic was added for the MIC assays. The 96-well plates were incubated at 37°C under static conditions in a Synergy™ NEOALPHAB multi-mode microplate reader (BioTek®, Winooski, VT, USA). Growth was monitored by changes in OD_{595}. For each strain, the MIC at 15 h was defined as the lowest antibiotic concentration where the final OD was at or below the starting OD. All experiments were performed at least in duplicate.

Microscopy

Stationary phase cell cultures assessed in MIC assays were photographed. Morphology of cultures grown for 24 h in MRS was taken as reference. Possible morphological changes on bacteria were checked after exposition for 24 h to BR005, BR080, BR081, BR087, BR088, BR090, BR091, BR092, subtilin and *H. illucens* larval extracts. The cells were observed in an Olympus AX70 microscope with phase contrast at 40x magnification. Pictures were taken with an Olympus U-TV1XC camera. Pictures were analysed using the tools implemented in the Olympus Cells Sens Dimensions 1.14 software and Corel Photo Paint X5.

The average cell length of the bacteria (n = 200), the average cell-chains length (n = 40 cell-chains) and the average number of cells per chain (n = 40 cell-chains) of the stationary phase cell cultures photographed were determined using the tools implemented in the ImageJ 1.52i software (61). Unpaired t-tests (two-tailed P value, 95% confidence intervals) comparing the values of BL23 and *ΔderB* under the reference condition indicated means significantly different ($P<0.05$) for the cell-chains length (P value= 0.023) and the number of cells per chain (P value= 0.002). To determine whether the morphological phenotypes of the mutant strain upon exposition to each insect derived AMP assayed were significantly different from that of the wild type, pairwise two-way ANOVA analyses were run with GraphPad Prism 5 software, testing the values of both strains under the reference condition and after each AMP exposition. A significant difference was considered when the analysis estimated P values were below of 0.01.

Cytochrome c binding assay

Comparison of the whole-cell surface charge of the wild-type strain and mutant *ΔderB* was performed by a cytochrome *c* binding assay as in (32). Briefly, cells in stationary phase at 10^{10} CFU ml^{-1} were incubated with 150 µg ml^{-1} cytochrome *c* (Sigma) in 20 mM MOPS (morpholinepropanesulfonic acid), pH 7, for 10 min at room temperature. The mixture was centrifuged twice, and the absorbance of the supernatant (containing unbound cytochrome *c*) was

506 determined at 530 nm. The binding ratio was calculated by comparing the absorbance of each
507 supernatant after incubation with the cells relative to the absorbance of the cytochrome *c* solution
508 without bacterial cells.

509 ***Antimicrobial peptide information and structure predictions***

510 The Antimicrobial Peptide Database (APD) (http://aps.unmc.edu/AP/main.php) (8) was
511 used as a reference for the information listed in Table 1. For structural information the Protein
512 Data Bank (www.rcsb.org) (62) or UniProt (http://www.uniprot.org/) (63) were used. The
513 structures of Plectasin (PDB ID 1ZFU (64)), BR080 (sapecin A; PDB ID 1L4V (65)) and BR088
514 (lucifensin, PDB ID 2LLD (66)) were used. If no structure was available, the Swiss-Model webpage
515 was used to generate structural predictions (https://swissmodel.expasy.org/) (67-70). The
516 structures of BR081, BR087, BR089, BR090, BR091 and BR092 were modelled applying the
517 Sapecin A structure (PDB: 1L4V) as template. Structural comparison was performed with YASARA
518 View (www.yasara.org) program. Multiple sequence alignment of the defensins was performed
519 with the CLC Main Workbench 7.7.3 program.

520 ***Reverse-transcription and quantitative real-time PCR (qRT-PCR)***

521 Samples for RNA isolation were collected as previously described (32). Nisin 22.5 ng ml^{-1}
522 and subtilin 1 % were used for the induction assays. Isolation of total RNA from *L. casei* strains,
523 synthesis of cDNA, primer design and qRT-PCR were carried out as described previously (71).
524 Primers used are listed in Table 4. *lepA*, *ileS*, *pyrG* and *pcrA* were used as constitutive reference
525 genes (71). Linearity and amplification efficiency for each primer pair were previously determined
526 (32). The relative expression based on the expression ratio between the target genes and
527 reference genes was calculated using the software tool REST (72). Every real-time PCR
528 determination was performed at least six times.

529

AKNOWLEDGMENTS:

This work was financially supported by the DFG grant MA2837/3-2 (to T.M.), and funds from the former Spanish Ministry of Science and Innovation and FEDER (AGL2010-15679) and the Generalitat Valenciana (ACOMP2012/137) (to M.Z.). A.R.-G. thanks the Federation of European Microbiological Societies for the Research Grant FEMS-RG-2014-0067. Q.Z. is financially supported by a stipend from the China Scholarship Council (CSC). A.M. thanks Herwig Gutzeit (TU Dresden) for his encouragement regarding the *Hermetia illucens* projects and Bio.S Biogas GmbH (Grimma, Germany), where *Hermetia illucens* cultures were maintained under the supervision of Dennis Hluschi.

The authors declare no conflict of interest.

AUTHORS CONTRIBUTIONS:

A.R.-G., M.Z. and T.M. conceived the study and planned the experiments. A.R-G analyzed the data and wrote the manuscript under the supervision of T.M.; M.Z. and S.G. contributed to discussing the results and the final manuscript. A.R.-G. carried out most of the experiments with *L. casei* and designed the B2H constructs; C.A. contributed to the construction of the mutant strains and the qRT-PCR experiments; Q.Z. performed the B2H cloning and experiments. C.L. performed the structural analysis of defensins and contributed to writing of the manuscript. A.M. prepared *H. illucens* larvae extracts. M.R and A. V. prepared insect derived AMPs. All authors read the paper and commented on the final manuscript.

REFERENCES

1. Ageitos JM, Sánchez-Pérez A, Calo-Mata P, Villa TG. 2016. Antimicrobial peptides (AMPs): Ancient compounds that represent novel weapons in the fight against bacteria. Biochem Pharmacol doi:10.1016/j.bcp.2016.09.018.
2. Hancock REW, Chapple DS. 1999. Peptide Antibiotics. Antimicrobial Agents and Chemotherapy 43:1317-1323.
3. Draper LA, Cotter PD, Hill C, Ross RP. 2015. Lantibiotic resistance. Microbiol Mol Biol Rev 79:171-91.
4. Perron GG, Zasloff M, Bell G. 2006. Experimental evolution of resistance to an antimicrobial peptide. Proc Biol Sci 273:251-6.
5. Brogden KA. 2005. Antimicrobial peptides: pore formers or metabolic inhibitors in bacteria? Nat Rev Micro 3:238-250.
6. Brötz H, Josten M, Wiedemann I, Schneider U, Götz F, Bierbaum G, Sahl HG. 1998. Role of lipid-bound peptidoglycan precursors in the formation of pores by nisin, epidermin and other lantibiotics. Mol Microbiol 30:317-27.
7. Oppedijk SF, Martin NI, Breukink E. 2016. Hit 'em where it hurts: The growing and structurally diverse family of peptides that target lipid-II. Biochim Biophys Acta 1858:947-57.
8. Wang G, Li X, Wang Z. 2015. APD3: the antimicrobial peptide database as a tool for research and education. Nucleic Acids Res doi:10.1093/nar/gkv1278.
9. McAuliffe O, Ross RP, Hill C. 2001. Lantibiotics: structure, biosynthesis and mode of action. FEMS Microbiol Rev 25:285-308.
10. Dias Rde O, Franco OL. 2015. Cysteine-stabilized alphabeta defensins: From a common fold to antibacterial activity. Peptides 72:64-72.
11. Yi HY, Chowdhury M, Huang YD, Yu XQ. 2014. Insect antimicrobial peptides and their applications. Appl Microbiol Biotechnol 98:5807-22.
12. Revilla-Guarinos A, Gebhard S, Mascher T, Zúñiga M. 2014. Defence against antimicrobial peptides: different strategies in Firmicutes. Environ Microbiol 16:1225-37.
13. Neuhaus FC, Baddiley J. 2003. A continuum of anionic charge: structures and functions of D-alanyl-teichoic acids in gram-positive bacteria. Microbiol Mol Biol Rev 67:686-723.
14. Neuhaus FC, Heaton MP, Debabov DV, Zhang Q. 1996. The *dlt* operon in the biosynthesis of D-alanyl-lipoteichoic acid in *Lactobacillus casei*. Microb Drug Resist 2:77-84.
15. Ernst CM, Peschel A. 2011. Broad-spectrum antimicrobial peptide resistance by MprF-mediated aminoacylation and flipping of phospholipids. Mol Microbiol 80:290-9.
16. Peschel A, Jack RW, Otto M, Collins LV, Staubitz P, Nicholson G, Kalbacher H, Nieuwenhuizen WF, Jung G, Tarkowski A, van Kessel KP, van Strijp JA. 2001. *Staphylococcus aureus* resistance to human defensins and evasion of neutrophil killing via the novel virulence factor MprF is based on modification of membrane lipids with l-lysine. J Exp Med 193:1067-76.
17. Gebhard S. 2012. ABC transporters of antimicrobial peptides in Firmicutes bacteria - phylogeny, function and regulation. Mol Microbiol 86:1295-317.
18. Mascher T, Margulis NG, Wang T, Ye RW, Helmann JD. 2003. Cell wall stress responses in *Bacillus subtilis*: the regulatory network of the bacitracin stimulon. Mol Microbiol 50:1591-604.
19. Ohki R, Giyanto, Tateno K, Masuyama W, Moriya S, Kobayashi K, Ogasawara N. 2003. The BceRS two-component regulatory system induces expression of the bacitracin transporter, BceAB, in *Bacillus subtilis*. Mol Microbiol 49:1135-44.
20. Dintner S, Heermann R, Fang C, Jung K, Gebhard S. 2014. A sensory complex consisting of an ATP-binding cassette transporter and a two-component regulatory system controls bacitracin resistance in Bacillus subtilis. J Biol Chem 289:27899-910.
21. Dintner S, Staroń A, Berchtold E, Petri T, Mascher T, Gebhard S. 2011. Coevolution of ABC transporters and two-component regulatory systems as resistance modules against antimicrobial peptides in *Firmicutes* Bacteria. J Bacteriol 193:3851-62.

22. Joseph P, Fichant G, Quentin Y, Denizot F. 2002. Regulatory relationship of two-component and ABC transport systems and clustering of their genes in the Bacillus/Clostridium group, suggest a functional link between them. J Mol Microbiol Biotechnol 4:503-13.
23. Kobras CM, Piepenbreier H, Emenegger J, Sim A, Fritz G, Gebhard S. 2020. BceAB-Type Antibiotic Resistance Transporters Appear To Act by Target Protection of Cell Wall Synthesis. Antimicrobial Agents and Chemotherapy 64:e02241-19.
24. Piepenbreier H, Sim A, Kobras CM, Radeck J, Mascher T, Gebhard S, Fritz G. 2020. From Modules to Networks: a Systems-Level Analysis of the Bacitracin Stress Response in *Bacillus subtilis*. mSystems 5:e00687-19.
25. Fritz G, Dintner S, Treichel NS, Radeck J, Gerland U, Mascher T, Gebhard S. 2015. A New Way of Sensing: Need-Based Activation of Antibiotic Resistance by a Flux-Sensing Mechanism. MBio 6:e00975.
26. Koh A, Gibbon MJ, Van der Kamp MW, Pudney CR, Gebhard S. 2020. How to make a dial not a switch: Control of histidine kinase conformation by an ABC-transporter facilitates need-based activation of antibiotic resistance. bioRxiv doi:10.1101/2020.02.28.969956:2020.02.28.969956.
27. Gebhard S, Fang C, Shaaly A, Leslie DJ, Weimar MR, Kalamorz F, Carne A, Cook GM. 2014. Identification and Characterization of a Bacitracin Resistance Network in *Enterococcus faecalis*. Antimicrobial Agents and Chemotherapy 58:1425-1433.
28. Gebhard S, Mascher T. 2011. Antimicrobial peptide sensing and detoxification modules: unravelling the regulatory circuitry of *Staphylococcus aureus*. Mol Microbiol 81:581-7.
29. Staroń A, Finkeisen DE, Mascher T. 2011. Peptide antibiotic sensing and detoxification modules of *Bacillus subtilis*. Antimicrob Agents Chemother 55:515-25.
30. Kallenberg F, Dintner S, Schmitz R, Gebhard S. 2013. Identification of regions important for resistance and signalling within the antimicrobial peptide transporter BceAB of *Bacillus subtilis*. J Bacteriol 195:3287-97.
31. Alcántara C, Revilla-Guarinos A, Zúñiga M. 2011. Influence of Two-Component Signal Transduction Systems of *Lactobacillus casei* BL23 on Tolerance to Stress Conditions. Appl Environ Microbiol 77:1516-1519.
32. Revilla-Guarinos A, Gebhard S, Alcántara C, Staroń A, Mascher T, Zúñiga M. 2013. Characterization of a Regulatory Network of Peptide Antibiotic Detoxification Modules in *Lactobacillus casei* BL23, 2013/03/05 ed doi:10.1128/AEM.00178-13.
33. Revilla-Guarinos A, Alcántara C, Rozès N, Voigt B, Zúñiga M. 2014. Characterization of the response to low pH of Lactobacillus casei ΔRR12, a mutant strain with low D-alanylation activity and sensitivity to low pH. J Appl Microbiol 116:1250-61.
34. Li M, Lai Y, Villaruz AE, Cha DJ, Sturdevant DE, Otto M. 2007. Gram-positive three-component antimicrobial peptide-sensing system. Proc Natl Acad Sci U S A 104:9469-74.
35. Heeney DD, Gareau MG, Marco ML. 2018. Intestinal *Lactobacillus* in health and disease, a driver or just along for the ride? Curr Opin Biotechnol 49:140-147.
36. Dommett R, Zilbauer M, George JT, Bajaj-Elliott M. 2005. Innate immune defence in the human gastrointestinal tract. Mol Immunol 42:903-12.
37. Hase K, Murakami M, Iimura M, Cole SP, Horibe Y, Ohtake T, Obonyo M, Gallo RL, Eckmann L, Kagnoff MF. 2003. Expression of LL-37 by human gastric epithelial cells as a potential host defense mechanism against *Helicobacter pylori*. Gastroenterology 125:1613-25.
38. Pietiäinen M, Gardemeister M, Mecklin M, Leskela S, Sarvas M, Kontinen VP. 2005. Cationic antimicrobial peptides elicit a complex stress response in *Bacillus subtilis* that involves ECF-type sigma factors and two-component signal transduction systems. Microbiology 151:1577-92.
39. Müller A, Wolf D, Gutzeit HO. 2017. The black soldier fly, *Hermetia illucens* - a promising source for sustainable production of proteins, lipids and bioactive substances. Z Naturforsch C 72:351-363.
40. Schroeder BO, Wu Z, Nuding S, Groscurth S, Marcinowski M, Beisner J, Buchner J, Schaller M, Stange EF, Wehkamp J. 2011. Reduction of disulphide bonds unmasks potent antimicrobial activity of human beta-defensin 1. Nature 469:419-23.

41. Zhao C, Wang I, Lehrer RI. 1996. Widespread expression of beta-defensin hBD-1 in human secretory glands and epithelial cells. FEBS Lett 396:319-22.
42. Matos RC, Leulier F. 2014. Lactobacilli-Host mutualism: "learning on the fly". Microb Cell Fact 13 Suppl 1:S6.
43. Singh B, Crippen TL, Zheng L, Fields AT, Yu Z, Ma Q, Wood TK, Dowd SE, Flores M, Tomberlin JK, Tarone AM. 2015. A metagenomic assessment of the bacteria associated with *Lucilia sericata* and *Lucilia cuprina* (*Diptera: Calliphoridae*). Appl Microbiol Biotechnol 99:869-83.
44. Rietkötter E, Hoyer D, Mascher T. 2008. Bacitracin sensing in *Bacillus subtilis*. Mol Microbiol 68:768-85.
45. Peschel A, Otto M, Jack RW, Kalbacher H, Jung G, Götz F. 1999. Inactivation of the *dlt* operon in *Staphylococcus aureus* confers sensitivity to defensins, protegrins, and other antimicrobial peptides. J Biol Chem 274:8405-10.
46. Park S-I, Chang BS, Yoe SM. 2014. Detection of antimicrobial substances from larvae of the black soldier fly, *Hermetia illucens* (Diptera: Stratiomyidae). Entomological Research 44:58-64.
47. Vogel H, Müller A, Heckel DG, Gutzeit H, Vilcinskas A. 2018. Nutritional immunology: Diversification and diet-dependent expression of antimicrobial peptides in the black soldier fly *Hermetia illucens*. Dev Comp Immunol 78:141-148.
48. Park SI, Kim JW, Yoe SM. 2015. Purification and characterization of a novel antibacterial peptide from black soldier fly (*Hermetia illucens*) larvae. Dev Comp Immunol 52:98-106.
49. Li Z, Mao R, Teng D, Hao Y, Chen H, Wang X, Yang N, Wang J. 2017. Antibacterial and immunomodulatory activities of insect defensins-DLP2 and DLP4 against multidrug-resistant *Staphylococcus aureus*. Sci Rep 7:12124.
50. Hammes WP, Hertel C. 2006. The Genera *Lactobacillus* and *Carnobacterium*. *In* Dr. MDP, Falkow S, Rosenberg E, Schleifer K-H, Stackebrandt E (ed), The Prokaryotes, vol Vol. 4. Springer US.
51. Boiocchi F, Porcellato D, Limonta L, Picozzi C, Vigentini I, Locatelli DP, Foschino R. 2017. Insect frass in stored cereal products as a potential source of *Lactobacillus sanfranciscensis* for sourdough ecosystem. J Appl Microbiol 123:944-955.
52. Radeck J, Gebhard S, Orchard PS, Kirchner M, Bauer S, Mascher T, Fritz G. 2016. Anatomy of the bacitracin resistance network in *Bacillus subtilis*. Mol Microbiol 100:607-20.
53. Kramer NE, van Hijum SA, Knol J, Kok J, Kuipers OP. 2006. Transcriptome analysis reveals mechanisms by which *Lactococcus lactis* acquires nisin resistance. Antimicrob Agents Chemother 50:1753-61.
54. Randall CP, Gupta A, Utley-Drew B, Lee SY, Morrison-Williams G, O'Neill AJ. 2018. Acquired Nisin Resistance in *Staphylococcus aureus* Involves Constitutive Activation of an Intrinsic Peptide Antibiotic Detoxification Module. mSphere 3.
55. Sambrook J, E. F. Fritsch, and T. Maniatis. . 1989. Molecular Cloning: a Laboratory Manual. Cold Spring Harbor Laboratory, Cold Spring Harbor, NY).
56. Holo H, Nes IF. 1989. High-Frequency Transformation, by Electroporation, of *Lactococcus lactis subsp. cremoris* Grown with Glycine in Osmotically Stabilized Media. Appl Environ Microbiol 55:3119-23.
57. Posno M, Leer RJ, van Luijk N, van Giezen MJ, Heuvelmans PT, Lokman BC, Pouwels PH. 1991. Incompatibility of *Lactobacillus* Vectors with Replicons Derived from Small Cryptic *Lactobacillus* Plasmids and Segregational Instability of the Introduced Vectors. Appl Environ Microbiol 57:1822-1828.
58. Schotte L, Steidler L, Vandekerckhove J, Remaut E. 2000. Secretion of biologically active murine interleukin-10 by *Lactococcus lactis*. Enzyme Microb Technol 27:761-765.
59. Karimova G, Pidoux J, Ullmann A, Ladant D. 1998. A bacterial two-hybrid system based on a reconstituted signal transduction pathway. Proc Natl Acad Sci U S A 95:5752-6.
60. Banerjee S, Hansen JN. 1988. Structure and expression of a gene encoding the precursor of subtilin, a small protein antibiotic. J Biol Chem 263:9508-14.

61. Schindelin J, Arganda-Carreras I, Frise E, Kaynig V, Longair M, Pietzsch T, Preibisch S, Rueden C, Saalfeld S, Schmid B, Tinevez J-Y, White DJ, Hartenstein V, Eliceiri K, Tomancak P, Cardona A. 2012. Fiji: an open-source platform for biological-image analysis. Nature Methods 9:676.
62. Berman HM, Westbrook J, Feng Z, Gilliland G, Bhat TN, Weissig H, Shindyalov IN, Bourne PE. 2000. The Protein Data Bank. Nucleic Acids Res 28:235-242.
63. TheUniProtConsortium. 2017. UniProt: the universal protein knowledgebase. Nucleic Acids Res 45:D158-D169.
64. Mygind PH, Fischer RL, Schnorr KM, Hansen MT, Sönksen CP, Ludvigsen S, Raventos D, Buskov S, Christensen B, De Maria L, Taboureau O, Yaver D, Elvig-Jorgensen SG, Sorensen MV, Christensen BE, Kjaerulff S, Frimodt-Moller N, Lehrer RI, Zasloff M, Kristensen HH. 2005. Plectasin is a peptide antibiotic with therapeutic potential from a saprophytic fungus. Nature 437:975-80.
65. Hanzawa H, Shimada I, Kuzuhara T, Komano H, Kohda D, Inagaki F, Natori S, Arata Y. 1990. 1H nuclear magnetic resonance study of the solution conformation of an antibacterial protein, sapecin. FEBS Letters 269:413-420.
66. Nygaard MK, Andersen AS, Kristensen HH, Krogfelt KA, Fojan P, Wimmer R. 2012. The insect defensin lucifensin from *Lucilia sericata*. J Biomol NMR 52:277-82.
67. Biasini M, Bienert S, Waterhouse A, Arnold K, Studer G, Schmidt T, Kiefer F, Cassarino TG, Bertoni M, Bordoli L, Schwede T. 2014. SWISS-MODEL: modelling protein tertiary and quaternary structure using evolutionary information. Nucleic Acids Res 42:W252-W258.
68. Arnold K, Bordoli L, Kopp J, Schwede T. 2006. The SWISS-MODEL workspace: a web-based environment for protein structure homology modelling. Bioinformatics 22:195-201.
69. Guex N, Peitsch MC, Schwede T. 2009. Automated comparative protein structure modeling with SWISS-MODEL and Swiss-PdbViewer: a historical perspective. Electrophoresis 30 Suppl 1:S162-73.
70. Kiefer F, Arnold K, Kunzli M, Bordoli L, Schwede T. 2009. The SWISS-MODEL Repository and associated resources. Nucleic Acids Res 37:D387-92.
71. Landete JM, García-Haro L, Blasco A, Manzanares P, Berbegal C, Monedero V, Zúñiga M. 2010. Requirement of the *Lactobacillus casei* MaeKR two-component system for L-malic acid utilization via a malic enzyme pathway. Appl Environ Microbiol 76:84-95.
72. Pfaffl MW, Horgan GW, Dempfle L. 2002. Relative expression software tool (REST) for group-wise comparison and statistical analysis of relative expression results in real-time PCR. Nucleic Acids Res 30:e36.
73. Wang G. 2015. Improved Methods for Classification, Prediction and Design of Antimicrobial Peptides. Methods in molecular biology (Clifton, NJ) 1268:43-66.
74. Gasson MJ. 1983. Plasmid complements of *Streptococcus lactis* NCDO 712 and other lactic streptococci after protoplast-induced curing. J Bacteriol 154:1-9.
75. Leloup L, Ehrlich SD, Zagorec M, Morel-Deville F. 1997. Single-crossover integration in the *Lactobacillus sake* chromosome and insertional inactivation of the *ptsI* and *lacL* genes. Appl Environ Microbiol 63:2117-23.

TABLES

Table 1: Antimicrobial peptides used in this study and MIC values against *L. casei* BL23 and *ΔderB*.

AMP		Class	AP Database ID[a]	Sequence	3D structure[b]	MIC[c] (15h)	
						BL23	*ΔderB*
Bacteriocins							
Bacitracin		cyclic peptide	n. r.	ICLEIKOrnIFHDN [d] (bond between Lys_6 and Asn_{12})	cyclic	10	10
Nisin A		type A lantibiotic	AP00205	ITSISLCTPGCKTGALMGCNMKTATCHCSIHVSK	non-αβ	**0.5**	**5**
Mersacidin		type B lantibiotic	AP01206	CTFTLPGGGGVCTLTSECIC	non-αβ	10	10
Subtilin		type A lantibiotic	AP00206	WKSESLCTPGCVTGALQTCFLQTLTCNCKISK	unknown	3[c]	3[c] **(¶)**
Vancomycin		glycopeptide	n. r.	n.f.	branched tricyclic	1.7[c]	1.7[c]
Fungi AMPs							
Plectasin		defensin	AP00549	GFGCNGPWDEDDMQCHNHCKSIKGYKGGYCAKGGFVCKCY	combine-αβ	**>40**	**>40 (¶)**
Insect AMPs							
BR001	Cecropin A	cecropin	AP00139	KWKLFKKIEKVGQNIRDGIIKAGPAVAVVGQATQIAK*-NH2	α	>320	>320
BR002	Sarcotoxin IA	cecropin A2	AP00230	GWLKKIGKKIERVGQHTRDATIQGLGIAQQAANVAATAR*-NH2	α	>320	>320
BR003	Cecropin A (insect: *Aedes aegypti*)	cecropin	n.r.	GGLKKLGKKLEGAGKRVFNAAEKALPVVAGAKALRK	(α)	>320	>320
BR005	Stomoxyn	stomoxyn	AP00484	RGFRKHFNKLVKKVKHTISETAHVAKDTAVIAGSGAAVVAAT	α	>320	>320
BR044	LSerStomox2	stomoxyn	AP02513	GFRKRFNKLVKKVKHTIKETANVSKDVAIVAGSGVAVGAAMG	(α)	>320	>320
BR080	Sapecin A	defensin	AP00227	ATCDLLSGTGINHSACAAHCLLRGNRGGYCNGKAVCVCRN	combine-αβ	**>160**	**80**
BR081	(insect: *Aeschna cyanea*)	defensin	AP00182	GFGCPLDQMQCHRHCQTITGRSGGYCSGPLKLTCTCYR	bridge	>320	>320
BR087	(insect: *Lucilia sericata*)	defensin	n. r.	ATCDLLSATGFSGTACAAHCLLIGHRGGYCNTKSVCVCRD	(combine-αβ)	>400	>400
BR088	Lucifensin	defensin	AP01532	ATCDLLSGTGVKHSACAAHCLLRGNRGGYCNGRAICVCRN	combine-αβ	>400	>400
BR089	LSer-Def7	defensin	AP02507	FTCNSYACKAHCILQGHKSGSCARINLCKCQR	bridge	>320	>320
BR090	LSer-Def4	defensin	AP02505	LTCNIDRSFCLAHCLLRGYKRGFCTVKKICVCRH	bridge	**>400**	**>400 (¶)**
BR091	LSer-Def6	defensin	AP02506	GTCSFSSALCVVHCRVRGYPDGYCSRKGICTCRR	bridge	>400	>400
BR092	LSer-Def3	defensin	AP02504	ATCDLLSGTGANHSACAAHCLLRGNRGGYCNSKAVCVCRN	bridge	**>320**	**320**
BR097	Cecropin A (*Galleria mellonella*)	cecropin	AP03067	KWKIFKKIEKAGRNIRDGIIKAGPAVSVVGEAATIYKTG*-NH2	(α)	>320	>320
BR098	Cecropin B (*G. mellonella*)	cecropin	AP03068	KWKFFKKIERVGQNIRDGIIKAGPAVQVVGQAATIYKGK*-NH2	(α)	>320	>320
BR099	Cecropin C (*G. mellonella*)	cecropin	AP03069	RWKVFKKIERMGQHIRDGIIKAGPAVAVVGQASTIISG*-NH2	(α)	>320	>320

BR100	Gm cecropin D-like pept	cecropin D	AP00755	ENFFKEIERAGQRIRDAIISAAPAVETLAQAQKIIKGGD*-NH2	(α)	>320	>320
BR101	Et-Cec1 (*Eristalis tenax*)	cecropin	n. r.	GFLKKIGKKLEGAVQRTRDATIQTIAVAQAAANVAATAKQG	(α)	>320	>320
Human AMPs							
LL37		cathelicidin	AP00310	LLGDFFRKSKEKIGKEFKRIVQRIKDFLRNLVPRTES	α-helix	>27	>27
hBD-1		defensin	AP00451	DHYNCVSSGGQCLYSACPIFTKIQGTCYRGKAKCCK	combine-αβ	>20	>20

[a] Antimicrobial Peptide Database (APD3) (8) identification number. n.r., not registered in APD3; n.f., not found. [b]3D structure as annotated in APD3 based in (73): **α**, AMPs with helical structures; **combine-αβ**, AMPs with α-helical and β-strands in the 3D structure; **non-αβ**, contains neither α-helical nor β-strands; **bridge**, AMPs without 3D structure determined, disulfide-linked, usually β-structure. When no structural data was available, structure prediction was made using the Swiss-Model webpage (https://swissmodel.expasy.org/) (67) and is indicated in parenthesis. [c]MIC in μg ml^{-1} except for: subtilin (% (v/v)) and vancomycin (mg/ml). **(¶)** indicates that the mutant is more sensitive when assays for final cell densities (see Fig. 2). [d] Sequence of linear peptide precursor.

749 **TABLE 2. Bacterial strains used in this study**

Strains	Description[a]	Source or reference
E. coli DH10β	F$^-$ *mcrA* Δ(*mrr-hsdRMS-mcrBC*) Φ80d*lacZ*Δ*M15* Δ*lacX74 endA1 recA1 deoR* Δ(*ara,leu*)7697 *araD139 galU galK nupG rpsL* λ$^-$	Stratagene
E. coli BTH101	F-, *cya-99, araD139, galE15, galK16, rpsL1 (Str^r), hsdR2, mcrA1, mcrB1.*	Lab collection
L. lactis MG1363	Plasmid-free derivative of NCDO712	(74)
L. casei BL23	Wild type	B. Chassy, U. Illinois
L. casei ΔpsdR	BL23 *ΔLCABL_16430*	(32)
L. casei ΔapsR	BL23 Δ*rrp1* (*LCABL_19600*)	(31)
L. casei ΔderB	BL23 *ΔLCABL_21670*	This study
L. casei C-ΔderB	BL23 *ΔLCABL_21670* harbouring plasmid *pT1*-RBS$_{derB}$*derB Ery^r*	This study
L. casei ΔpsdB	*LCABL_16400* mutant; *pRV16400 Ery^r*	(32)
L. casei ΔapsB	*LCABL_19580* mutant; *pRV19580 Ery^r*	(32)
L. casei ΔdltA	*LCABL_08550 (dltA)* mutant*; pRV08550 Ery^r*	(32)
L. casei ΔmprF	*LCABL_24490* mutant; *pRV24490 Ery^r*	(32)
L. casei ΔderBΔpsdB	BL23 *ΔLCABL_21670*; *LCABL_16400* mutant, *pRV16400 Ery^r*	This study
L. casei ΔderBΔdltA	BL23 *ΔLCABL_21670*; *LCABL_08550 (dltA)* mutant, *pRV08550 Ery^r*	This study

750 [a] *Amp^r*, ampicillin resistance; *Ery^r*, erythromycin resistance; *Str^r*, streptomycin resistance.

751

752 **TABLE 3. Vectors and plasmids used in this study**

Vector or plasmid	Description[a]	Source or reference
pRV300	Insertional vector for *Lactobacillus*, *Amp*^{r}, *Ery*^{r}	(75)
pT1NX	Expression vector for Gram-positive bacteria harboring the constitutive P1 promoter; *Ery*^{r}	(58)
pRVOrPe-del	*pRV300* containing fused flanking fragments upstream and downstream of *LCABL_21670*	This study
pRV08550	*pRV300* containing a 679-pb internal fragment of *LCABL_08550* (*dltA*)	(32)
pRV16400	*pRV300* containing a 975-pb internal fragment of *LCABL_16400* (*psdB*)	(32)
pT1-RBS$_{derB}$*derB*	*pT1NX* with cloned *LCABL_21670* (*derB*) and its ribosome binding site (*derA-derB* 12 pb intergenic region)	This study
pUT18	Vector for B2H, *Amp*^{r}	Euromedex, BACTH System Kit Manual
pUT18C	Vector for B2H, *Amp*^{r}	
pUT18C zip	Control plasmid for B2H, *Amp*^{r}	
pKT25	Vector for B2H, *Kan*^{r}	
pKNT25	Vector for B2H, *Kan*^{r}	
pKT25 zip	Control plasmid for B2H, *Kan*^{r}	
pUT18C-HK9	*pUT18C* containing histidine kinase *psdS LCABL_16420*	This study
pKT25-HK9	*pKT25* containing histidine kinase *psdS LCABL_16420*	This study
pU-HK9-T18	*pUT18* containing histidine kinase *psdS LCABL_16420*	This study
pKN-HK9-T25	*pKNT25* containing histidine kinase *psdS LCABL_16420*	This study
pUT18C-RR9	*pUT18C* containing response regulator *psdR LCABL_16430*	This study
pKT25-RR9	*pKT25* containing response regulator *psdR LCABL_16430*	This study
pU-RR9-T18	*pUT18* containing response regulator *psdR LCABL_16430*	This study
pKN-RR9-T25	*pKNT25* containing response regulator *psdR LCABL_16430*	This study
pUT18C-Per9	*pUT18C* containing permease *psdB LCABL_16400*	This study
pKT25-Per9	*pKT25* containing permease *psdB LCABL_16400*	This study
pU-Per9-T18	*pUT18* containing permease *psdB LCABL_16400*	This study
pKN-Per9-T25	*pKNT25* containing permease *psdB LCABL_16400*	This study
pUT18C-ATP9	*pUT18C* containing ATPase *psdA LCABL_16410*	This study
pKT25-ATP9	*pKT25* containing ATPase *psdA LCABL_16410*	This study

pU-ATP9-T18	*pUT18* containing ATPase *psdA LCABL_16410*	This study
pKN-ATP9-T25	*pKNT25* containing ATPase *psdA LCABL_16410*	This study
pUT18C-HK12	*pUT18C* containing histidine kinase *apsS LCABL_19610*	This study
pKT25-HK12	*pKT25* containing histidine kinase *apsS LCABL_19610*	This study
pU-HK12-T18	*pUT18* containing histidine kinase *apsS LCABL_19610*	This study
pKN-HK12-T25	*pKNT25* containing histidine kinase *apsS LCABL_19610*	This study
pUT18C-RR12	*pUT18C* containing response regulator *apsS LCABL_19600*	This study
pKT25-RR12	*pKT25* containing response regulator *apsS LCABL_19600*	This study
pU-RR12-T18	*pUT18* containing response regulator *apsS LCABL_19600*	This study
pKN-RR12-T25	*pKNT25* containing response regulator *apsS LCABL_19600*	This study
pUT18C-Per12	*pUT18C* containing permease *apsB LCABL_19580*	This study
pKT25-Per12	*pKT25* containing permease *apsB LCABL_19580*	This study
pU-Per12-T18	*pUT18* containing permease *apsB LCABL_19580*	This study
pKN-Per12-T25	*pKNT25* containing permease *apsB LCABL_19580*	This study
pUT18C-ATP12	*pUT18C* containing ATPase *apsA LCABL_19590*	This study
pKT25-ATP12	*pKT25* containing ATPase *apsA LCABL_19590*	This study
pU-ATP12-T18	*pUT18* containing ATPase *apsA LCABL_19590*	This study
pKN-ATP12-T25	*pKNT25* containing ATPase *apsA LCABL_19590*	This study
pUT18C-OrPe	*pUT18C* containing permease *derB LCABL_21670*	This study
pKT25-OrPe	*pKT25* containing permease *derB LCABL_21670*	This study
pU-OrPe-T18	*pUT18* containing permease *derB LCABL_21670*	This study
pKN-OrPe-T25	*pKNT25* containing permease *derB LCABL_21670*	This study
pUT18C-OrATP	*pUT18C* containing ATPase *derB LCABL_21680*	This study
pKT25-OrATP	*pKT25* containing ATPase *derB LCABL_21680*	This study
pU-OrATP-T18	*pUT18* containing ATPase *derB LCABL_21680*	This study
pKN-OrATP-T25	*pKNT25* containing ATPase *derB LCABL_21680*	This study

753 [a] Amp^r, ampicillin resistance; Ery^r, erythromycin resistance; Kan^r, kanamycin resistance.

754

755

756

757 **Table 4. Primers used in this study**

Primer	Gene	Sequence (5´- 3´) [a]
Cloning		
RG037	LCABL_08550	AGTCAAGCTTGTTCAGATTATTCGCGCACC
RG038	LCABL_08550	GACTACTAGTCTGACACTTGATTGCCTTGC
RG047	LCABL_16400	**CTATAGGGCGAATTG**GGTACCGCAAGCCTTCAGTATCGCCG
RG048	LCABL_16400	**CTCGAGGGGGGGCCC**GGTACCTCAGCCGCGTTTTGATAGCG
RG062	LCABL_21680	TTTTCTCGAGTCAGGTTCAGGGAAAACGAC
RG063	LCABL_21680	GTGCGACCTAAAGGATCTTTTCTAGACGACGCCCCTTACTTTTG
RG064	Intergenic region LCABL_21670 and LCABL_21660	CAAAAGTAAGGGGCGTCGTCTAGAAAAGATCCTTTAGGTCGCAC
RG065	LCABL_21660	AAAAGAATTCCGCCTCAAAAGACTTCATGC
RG220	LCABL_21670	AAAAACTAGTTTAGGCTTTTTCCGCTAAGTTCTTATTG
RG221	LCABL_21670	AAAAAGATCTGGGGCGTCGTCTATGTTAACG
Cloning checking		
pRV300.fw	pRV300 vector	GTTTTCCCAGTCACGAC
pRV300.rv	pRV300 vector	CAGGAAACAGCTATGAC
pT1NX.fwd	pT1NX vector	TGGATTGGATTAGTTCTTGTGG
pT1NX.rev	pT1NX vector	CTTCTCTGTCGCTATCTGTTG
RG068	LCABL_21660	TATGAAGTCGGCTTCCCGCATG
RG069	LCABL_21680	GTGAATTCGTCGGCATCATG
RG076	LCABL_21680	AACACCCGCATTGAAAGGTG
RG077	LCABL_21660	TCAGCAAAAACGTCACTGGC
LSEI1418R	LCABL_16410	GTCAACATTACTTAAATTAAAAA
qRT-PCR		
lepA-F	lepA	CACATTGATCACGGGAAGTC
lepA-R	lepA	GTAATGCCACGTTCACGTTC
ileS-F	ileS	ACCATTCCGGCTAACTATGG
ileS-R	ileS	TCAGGATCTTCGGATTTTCC
pcrA-F	pcrA	CGGCCAATAATGTGATTCAG
pcrA-R	pcrA	TCATCAGTTTCGCTTTGAGC
pyrG-F	pyrG	AATTGCGCTTTTCACTGATG
pyrG-R	pyrG	CGAAATGATCGACCACAATC
RG006	LCABL_19580	GGGAACGCGCATTCATTGTG
RG007	LCABL_19580	TCTCGCGCTGAACAAGATCC
RG008	LCABL_21670	TTGCCGGTATTTTGGTCGGG
RG009	LCABL_21670	ATGTCCACAATACGGCTGGC
RG019	LCABL_08550	TGGTCGAGGTTTTCTTGGGC
RG020	LCABL_08550	CCGGTGTATGGGCAACATCC
RG021	LCABL_24490	GCCGGATCAGCCAAGACTTG
RG022	LCABL_24490	TTAGCATCGGTGTAACGGCG
RG027	LCABL_19590	TAGCTTTCAGGTCAACGCGG
RG028	LCABL_19590	CTTGGCGTCTCAATCGTTGC
RG029	LCABL_19600	GGCAATGAATATGGGCGCTG
RG030	LCABL_19600	TAGGTTCGTCGAAGCAAGGC
RG031	LCABL_21680	CACCCGCATTGAAAGGTGTC
RG032	LCABL_21680	GCAAGGTCGTTTTCCCTGAAC
RG033	LCABL_16410	GGACAGGATCTGAGCAACGTC
RG034	LCABL_16410	ATTGAAGGTGTCAAGCAAGTCG

	RG054	LCABL_16400	GTACCGTCCTTTCCCGCATC
	RG055	LCABL_16400	CCGATGGTAATGATCCCGGC
	RG056	LCABL_16430	AGCGAGTTACGCAAACACAG
	RG057	LCABL_16430	CGGCTCCTAAGTTCATCGCC
B2H			
	TM1220	pUT18 fwd	AGCTCACTCATTAGGCACCC
	TM1221	pUT18 rev	CCGTCGTAGCGGAACTGGCG
	TM1222	pUT18C fwd	TCGACGATGGGCTGGGAGCC
	TM1223	pUT18C rev	AGCAGACAAGCCCGTCAGGG
	TM1224	pKT25 fwd	GGCGGATATCGACATGTTCG
	TM1225	pKT25 rev	ATCGGTGCGGGCCTCTTCGC
	TM1226	pKT25N fwd	GCTCACTCATTAGGCACCCC
	TM1227	pKT25N rev	GGCGGAACATCAATGTGGCG
	TM5702	HK9-B2H-XbaI.fw1	AAAATCTAGAGATGATGAAAGCTTATTGCCGCTCG
	TM5703	HK9- B2H-SmaI.rv1	AAAACCCGGGTTACTCCACTTGCCACCGCG
	TM5704	HK9-B2H-SmaI.rv2	AAAACCCGGGGCTCCACTTGCCACCGCGTTTG
	TM5705	RR9-B2H-XbaI.fw1	AAAATCTAGAGATGGCACAGAAAATTTTTATTGTCGAAG
	TM5706	RR9-B2H-SmaI.rv1	AAAACCCGGGTCATGGCTTTGGTCCCTCAC
	TM5707	RR9-B2H-SmaI.rv2	AAAACCCGGGGTGGCTTTGGTCCCTCACTTGC
	TM5708	ATP9-B2H-XbaI.fw1	AAAATCTAGAGATGTCAACATTACTTAAATTAAAAAATATCGA AAAAAC
	TM5709	ATP9-B2H-BamHI.rv1	AAAAGGATCCTCTCATTGTCCATCGCCTGCCTTTG
	TM5710	ATP9-B2H-BamHI.rv2	AAAAGGATCCTCTTGTCCATCGCCTGCCTTTG
	TM5711	Per9-B2H-XbaI.fw1	AAAATCTAGAGATGAAATTCTACTTTAAGCTCGCTGC
	TM5712	Per9-B2H-SmaI.rv1	AAAACCCGGGTTAGCTGCGACTGGTAGCTTGG
	TM5713	Per9-B2H-SmaI.rv2	AAAACCCGGGGGCTGCGACTGGTAGCTTGGC
	TM6396	HK12-B2H-XbaI.fw1	AAAATCTAGAGATGCGGTTTCGTGATTATTTAAAGG
	TM6397	HK12-B2H-SmaI.rv1	AAAACCCGGGTCAGCTGTCTGGATGTGACCTAG
	TM6398	RR12-B2H-XbaI.fw1	AAAATCTAGAGGTGTTTAAAATCATGATCGTAGAGG
	TM6399	RR12-B2H-SmaI.rv1	AAAACCCGGGCTAAGGAACGATGTAACCTTGTC
	TM6400	P12-B2H-XbaI.fw1	AAAATCTAGAGGTGGAGGAGGCCATACCCGTG
	TM6401	P12-B2H-SmaI.rv1	AAAACCCGGGCTAATCAATCGCCCAACGGGAAAC
	TM6402	A12-B2H-XbaI.fw1	AAAATCTAGAGATGGCAATTCTTGAAGTATCTAACTTGAG
	TM6403	A12-B2H-SmaI.rv1	AAAACCCGGGTTAATCAGATGCCACACGGG
	TM6404	OrPe-B2H-XbaI.fw1	AAAATCTAGAGATGTTAACGAAACTTGCACTCGG
	TM6405	OrPe-B2H-BamHI.rv1	AAAAGGATCCTTAGGCTTTTTCCGCTAAGTTCTTATTG
	TM6406	OrA-B2H-XbaI.fw1	AAAATCTAGAGATGGACAAGCAACCTGTCGTAAC
	TM6407	OrA-B2H-BamHI.rv1	AAAAGGATCCTTACTTTTGAAATGTGCCGAGTGTG
	TM6408	HK12-B2H-SmaI.rv2	AAAACCCGGGGGCTGTCTGGATGTGACCTAGTCTG
	TM6409	RR12-B2H-SmaI.rv2	AAAACCCGGGGAGGAACGATGTAACCTTGTCC
	TM6410	P12-B2H-SmaI.rv2	AAAACCCGGGGATCAATCGCCCAACGGGAAACAG
	TM6411	A12-B2H-SmaI.rv2	AAAACCCGGGGATCAGATGCCACACGGGTATG
	TM6412	OrPe-B2H-BamHI.rv2	AAAAGGATCCTCGGCTTTTTCCGCTAAGTTCTTATTG
	TM6413	OrA-B2H-BamHI.rv2	AAAAGGATCCTCCTTTTGAAATGTGCCGAGTGTG

[a] Restriction sites are underlined. Sequences highlighted in boldface type are the sequences for the CloneEZ PCR reaction as in reference (32).

761 **FIGURES**

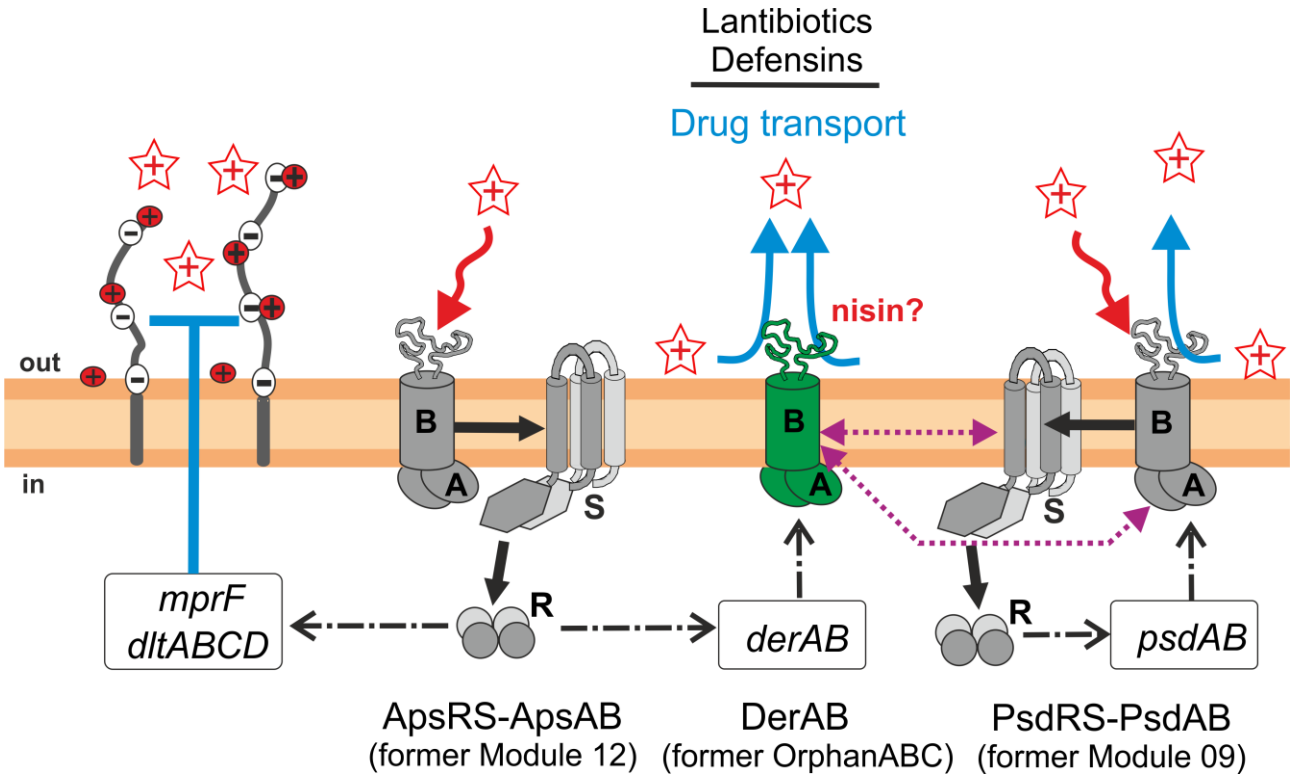

762

763 **Figure 1: Different layers of resistance against AMPs in *L. casei* BL23.**

764 ApsRSAB is a sensory module that regulates different layers of resistance against numerous AMPs.
765 The primary layer of AMP resistance is mediated by DerAB (drug transport) and the secondary
766 layer of resistance is mediated by the Dlt-system and MprF protein (drug repulsion). Resistance
767 mediated by DerAB is specific for defensins and – to a lesser degree - lantibiotics (see text for
768 details). PsdRSAB is a dual-function module involved in sensing and transport of various AMPs.

769 AMPs are depicted as red positively charged starts. S, histidine kinase; R, response regulator; B,
770 permease; A, ATPase. Homodimers of HKs and RRs are indicated. ABC transporters are composed
771 of a permease subunit and two ATPase domains (20). Signaling between the permeases and the
772 HKs and between the HKs and the RRs is indicated by black solid arrows. Gene activation and the
773 increased production of the transporters is indicated by black dash-dot arrows. Wave-shaped,
774 downward red arrows indicate sensing of AMPs; blue up-facing arrows indicate transport and
775 detoxification. B2H protein-protein interactions of DerB with PsdRSAB are indicated with purple
776 dotted lines. Lipoteichoic acids are indicated with grey negatively charged lines; D-alanylation of
777 teichoic acids and L-lysinilation of membrane phospholipids is indicated with positive red-filled
778 spheres; AMP charge-repulsion is indicated with a bar-headed up-facing blue line.

779

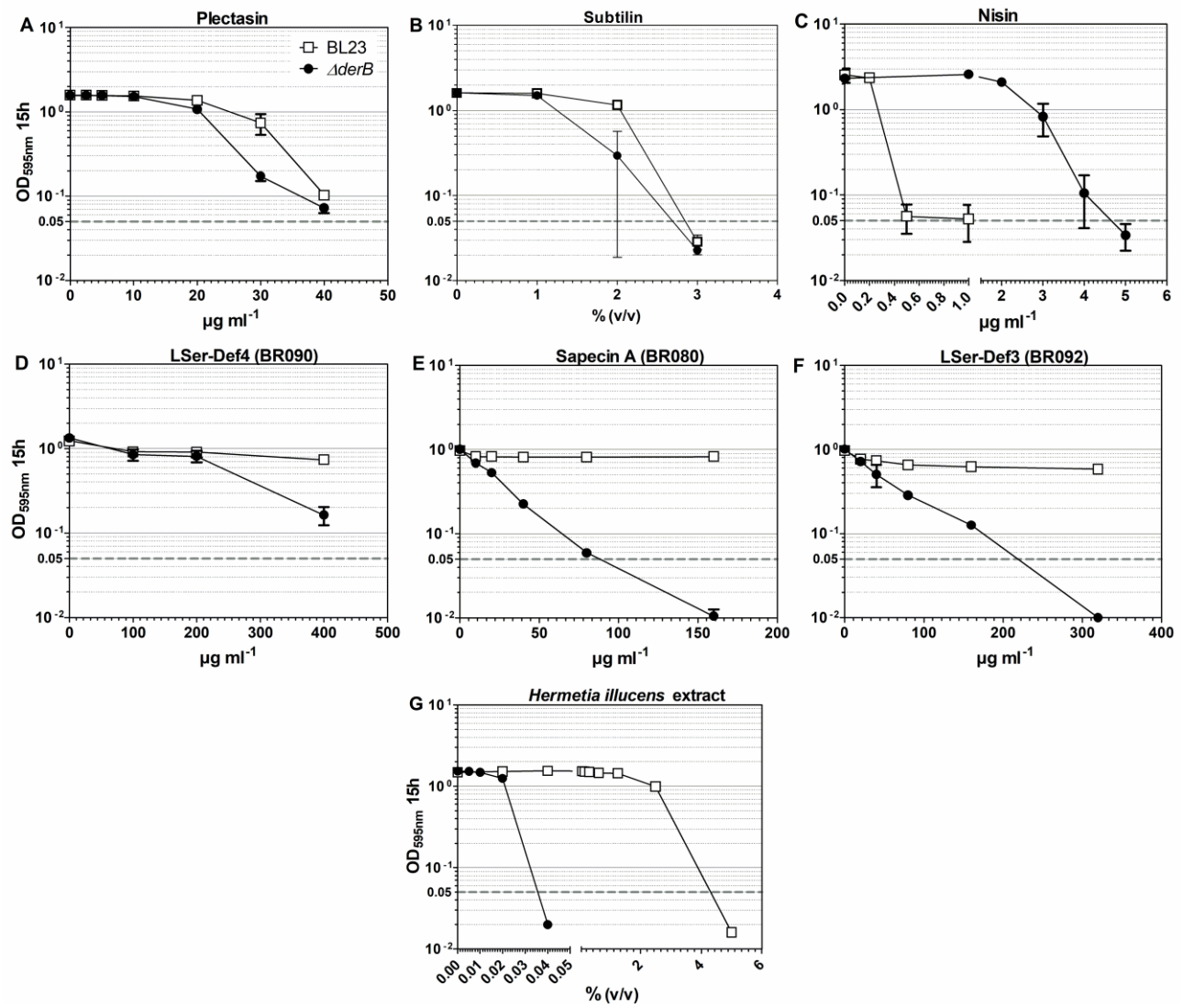

780

781 **Figure 2: MIC of different AMPs for *L. casei* BL23 (white squares) and *ΔderB* strains (black**
782 **circles). (A)** Plectasin. **(B)** Subtilin. **(C**) Nisin. **(D)** LSer-Def4 (BR090). **(E)** Sapecin A (BR080). **(F)** LSer-
783 Def3 (BR092). **(G)** Extract from *H. illucens* larvae. Strains were inoculated to an OD_{595} of 0.05
784 (dashed line) in MRS with different concentrations of antibiotics. Final OD_{595} readings were taken
785 after 15h incubation at 37°C (OD_{595} 15h). MIC (see Table 1) was defined at the lowest antibiotic
786 concentration where the final OD was at or below the starting OD. Mean and standard deviation
787 are presented of at least duplicates. A representative result of *H. illucens* extract is presented
788 because due to the preparation procedure, the absolute potency of each extract (as expressed in
789 %) varies significantly between individual preparations, but the relative sensitivities were very well
790 reproduced in independent assays.

791

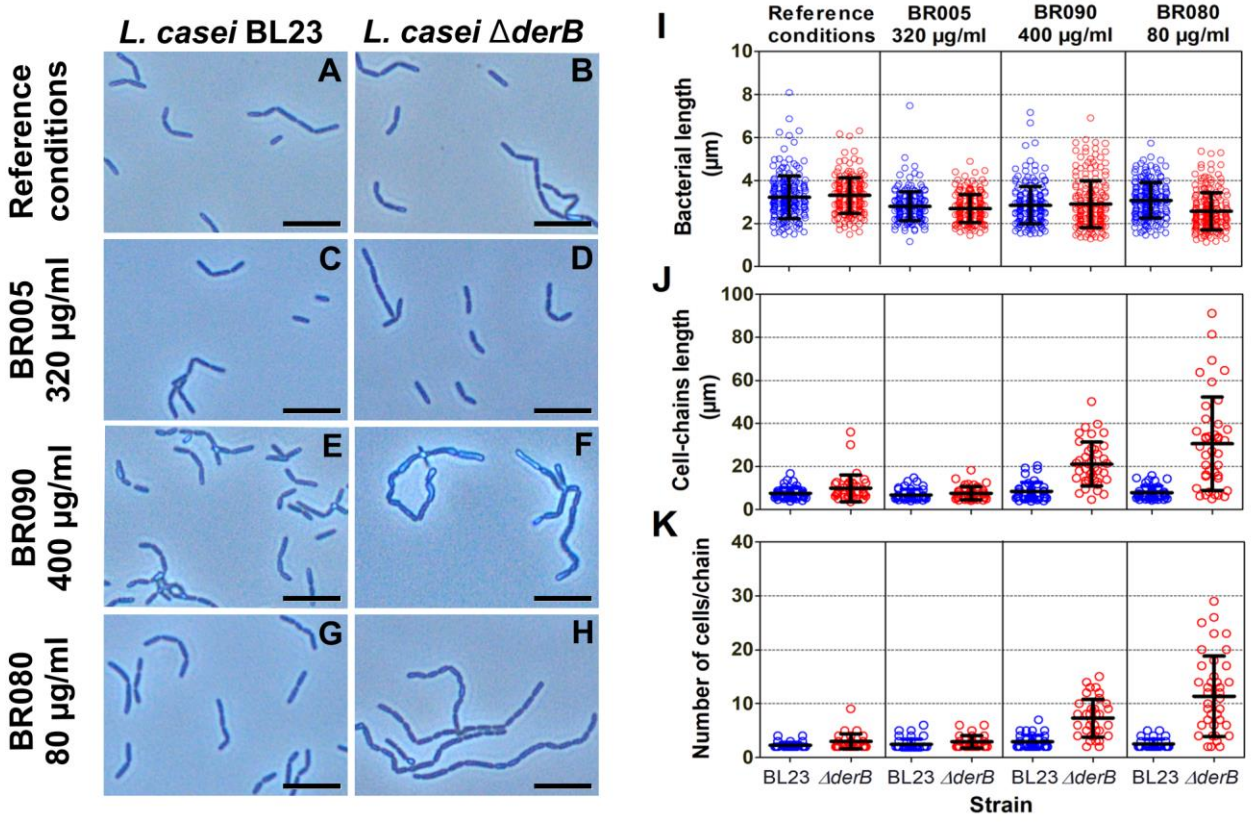

Figure 3: Sensitivity phenotypes of *ΔderB* strain are associated to morphological changes.
(A - H) Microscopic characterization after AMP exposition: stationary phase cell cultures of BL23 (left column pictures) and *ΔderB* (right column pictures) grown for 24 hours under reference conditions **(A and B)** or in the presence of insect derived AMPs were photographed (phase contrast, 40x magnification). Selected AMPs were chosen as representative of different sensitivities of the *ΔderB* strain relative to the wild type (see Table 1). Similar sensitivity phenotype: BR005 at 320 µg ml^{-1} **(C and D)**. *ΔderB* slightly more sensitive than BL23: BR090 at 400 µg ml^{-1} **(E and F)**. Mutant much more sensitive than wild type: BR080 at 80 µg ml^{-1} **(G and H)**. Scale bar 10 µm.
(I - K) Quantification of the morphological changes associated to the sensitivity phenotypes. **(I)**The average bacterial length (µm; n = 200), **(J)** the average cell-chains length (µm; n = 40 cell-chains) and **(K)** the average number of cells per chain (n = 40 cell-chains) of the stationary phase cell cultures photographed in **(A - H)** were determined. BL23 and *ΔderB* are depicted with blue and red circles, respectively. Means and standard deviations are indicated with the horizontal and the bar-headed vertical black lines, respectively. For a detailed statistical analysis of the results see Supplemental Table 1.

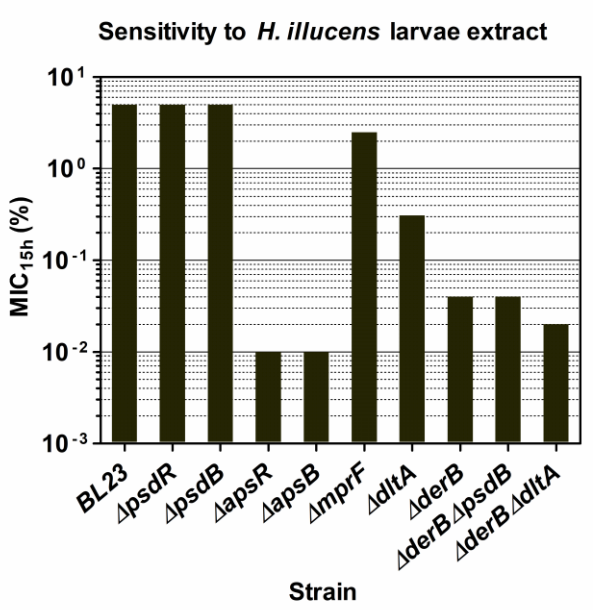

811

812 **Figure 4: Different layers of resistance against AMPs from *H. illucens*.** MIC at 15h (expressed as
813 % (v/v) of initial extract) of *H. illucens* larvae extract against *L. casei* BL23 and derivative strains. A
814 representative dataset is shown. Due to the preparation procedure, the absolute potency of each
815 extract (as expressed in %) vary significantly between individual preparations, but the overall
816 relative sensitivities were very well reproduced in independent assays.

817

818

819

820

821

822

823

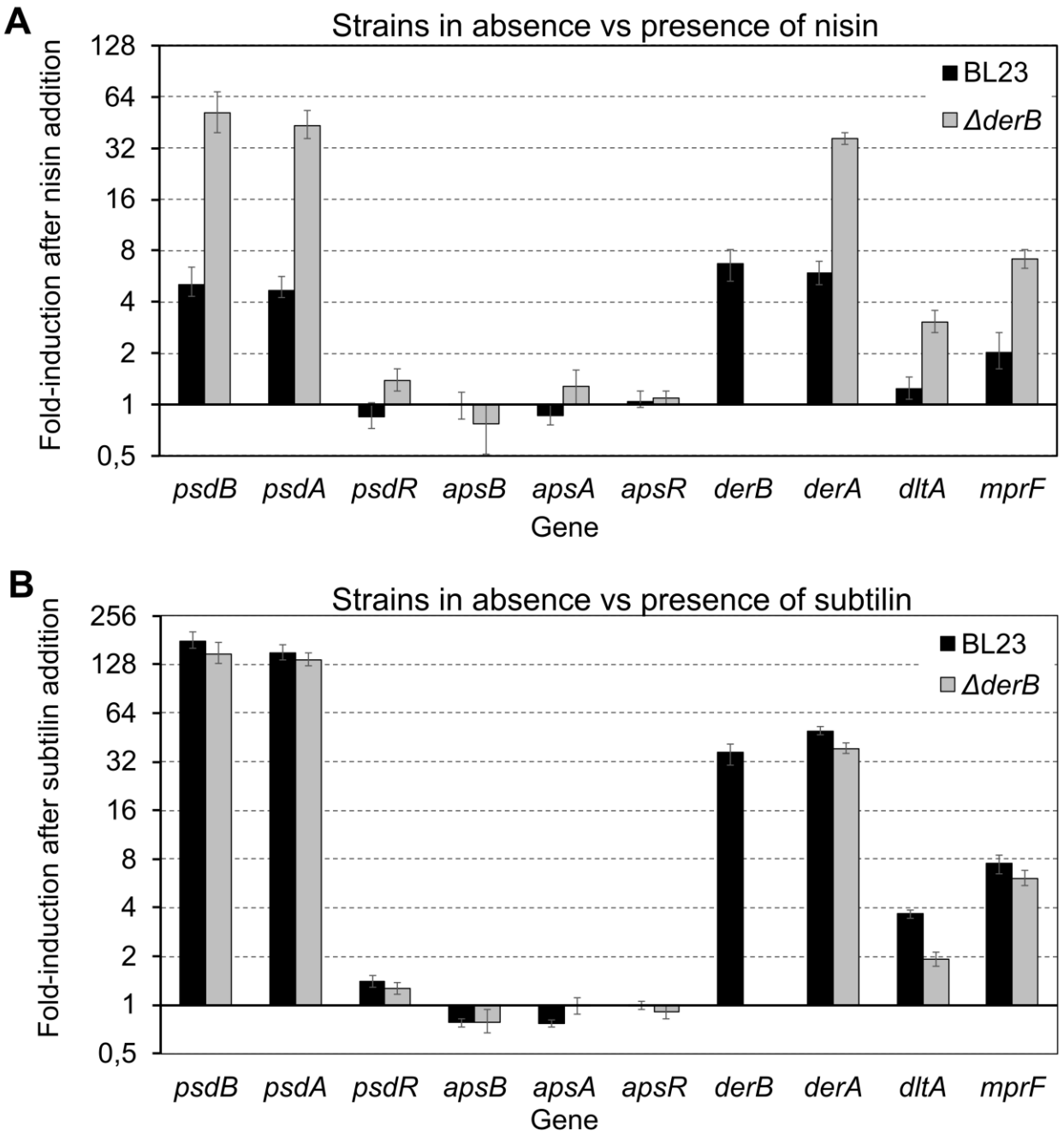

824

825 **Figure 5: Expression of known AMP resistance determinants in *L. casei* BL23 and *ΔderB* mutant**
826 **after nisin (A) and subtilin (B) addition.** Transcript levels were determined by real-time RT-PCR
827 10 min after addition of 22.5 ng ml^{-1} nisin **(A)** and 1% subtilin **(B)**. X-fold induction was calculated
828 relative to transcript levels in the same strain under reference conditions. Data are shown as mean
829 ± standard error of at least six replicates.

830

831

832

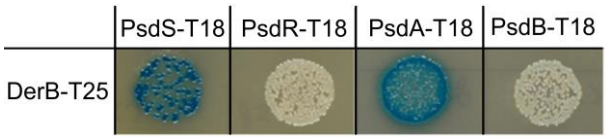

Figure 6: Bacterial two-hybrid analysis of the interactions of DerB with the PsdRSAB module. C-terminal and N-terminal translational fusions of the T18 and T25 domains of the adenylate cyclase CyaA of *B. pertussis* were created for each protein individually. Different hybrid fusions were tested in pairwise combinations in *E. coli* BTH101. The cells were spotted onto LB plates containing X-Gal (100 µg ml^{-1}), IPTG (1 mM), and antibiotics for selection. Pictures were taken after 48 h of incubation at 30 °C. The blue colonies indicate positive interaction results. For clarity, only a single representative pair is shown in the figure. See Figure S6 for the complete set of combinations.

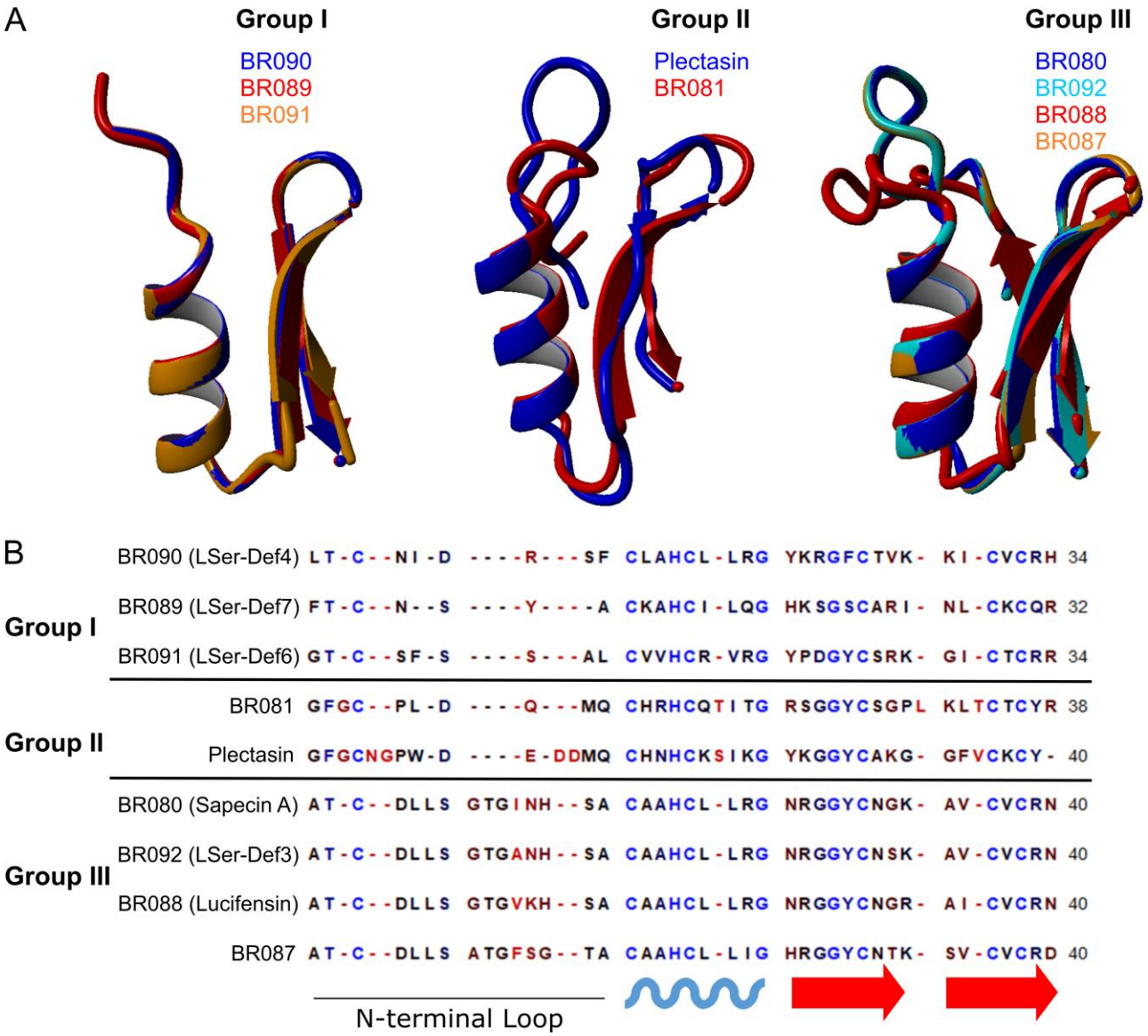

Figure 7: Structure and sequence comparison of defensins grouped according to loop size and loop sequence similarity. A) Structural alignment of defensins. Substrates of DerAB transporter are colored blue and cyan, non-substrates are colored red and orange. **B)** Sequence alignment. Residues are colored according to conservation from 0% (red) to 100% (blue). The N-terminal loop and the secondary structure elements (α-helix, blue wave and β-sheet, red arrows) are indicated under the alignment.

The ABC transporter DerAB of *Lactobacillus casei* mediates resistance against eukaryotic defensins

SUPPLEMENTAL MATERIAL

Ainhoa Revilla-Guarinos [1,#], Qian Zhang [1], Christoph Loderer[1], Cristina Alcántara [2], Ariane Müller[3], Mohammad Rahnamaeian[4], Andreas Vilcinskas[4,5], Susanne Gebhard[6], Manuel Zúñiga [2] and Thorsten Mascher [1,#]

[1] Institut für Mikrobiologie, Technische Universität Dresden, Dresden, Germany

[2] Instituto de Agroquímica y Tecnología de Alimentos (IATA-CSIC), Valencia, Spain

[3] Institut für Zoologie, Technische Universität Dresden, Dresden, Germany

[4] Fraunhofer Institute for Molecular Biology and Applied Ecology, Department of Bioresources, Giessen, Germany

[5] Institute for Insect Biotechnology, Justus Liebig University Giessen, Giessen, Germany

[6] Department of Biology and Biochemistry, Milner Centre for Evolution, University of Bath, United Kingdom

RUNNING TITLE: **Defensin resistance in *L. casei***

[#]Address correspondence to Ainhoa Revilla-Guarinos, ainhoa.revilla-guarinos@tu-dresden.de; or to Thorsten Mascher, thorsten.mascher@tu-dresden.de.

KEY WORDS: cell envelope stress response, antimicrobial peptide resistance, ABC transporter, two-component system, defensin, nisin

Supplemental Table 1. Quantification of the different sensitivity phenotypes of *L. casei* BL23 and *ΔderB* strains after exposition to insect derived AMPs. Stationary phase cell cultures of BL23 and *ΔderB* grown for 24 hours under reference conditions or in the presence of insect derived AMPs were photographed (see Figure 3 in the main text). The bacterial length, cell-chain length and number of cells per chain values were measured for each strain under the reference and stress conditions. Pairwise two-way ANOVA statistical analysis were applied to determine the contribution of the treatment and the strain to the morphological phenotypes (see Materials and methods in the main text for further details).

		Strain		ANOVA[d]		
Condition	Phenotype	BL23	*ΔderB*	Cond.	Strain	Int.
Reference conditions	Bacterial length (µm) [a, b]	3,22 ± 1,00	3,30 ± 0,83			
	Cell-chain length (µm) [a, c]	7,43 ± 2,74	9,92 ± 6,19			
	Number of cells/chain [a, c]	2,25 ± 0,54	3,03 ± 1,39			
BR005 320 µg/ml	Bacterial length (µm) [a, b]	2,80 ± 0,68	2,69 ± 0,64	**< 0,0001**	0,8318	0,0929
	Cell-chain length (µm) [a, c]	6,82 ± 2,65	7,59 ± 3,12	0,0200	0,0100	0,1711
	Number of cells/chain [a, c]	2,45 ± 1,01	2,9 ± 1,15	0,8362	**0,0004**	0,3304
BR090 400 µg/ml	Bacterial length (µm) [a, b]	2,85 ± 0,87	2,90 ± 1,10	**< 0,0001**	0,3104	0,8299
	Cell-chain length (µm) [a, c]	8,37 ± 4,22	21,1 ± 10,2	**< 0,0001**	**< 0,0001**	**< 0,0001**
	Number of cells/chain [a, c]	2,93 ±1,25	7,30 ± 3,55	**< 0,0001**	**< 0,0001**	**< 0,0001**
BR080 80 µg/ml	Bacterial length (µm) [a, b]	3,07 ± 0,83	2,57 ± 0,86	**< 0,0001**	**0,0008**	**< 0,0001**
	Cell-chain length (µm) [a, c]	7,82 ± 3,13	30,6 ± 21,7	**< 0,0001**	**< 0,0001**	**< 0,0001**
	Number of cells/chain [a, c]	2,55 ± 0,90	11,4 ± 7,46	**< 0,0001**	**< 0,0001**	**< 0,0001**

[a] The values represent means and standard deviations. [b] For bacterial length determination, n = 200 cells per condition; [c] for the determination of the cell-chain length and the number of cells per chain, n = 40 cell-chains per condition. [d] P values from pairwise two-way ANOVA analyses testing the growth of BL23 and *derB* mutant strain under the reference condition and in the presence of each of the three AMPs (BR005, BR090 and BR080) characterized microscopically in Figure 3. Significant differences (P value <0.01) are indicated in bold characters. Cond., condition; Int., interaction.

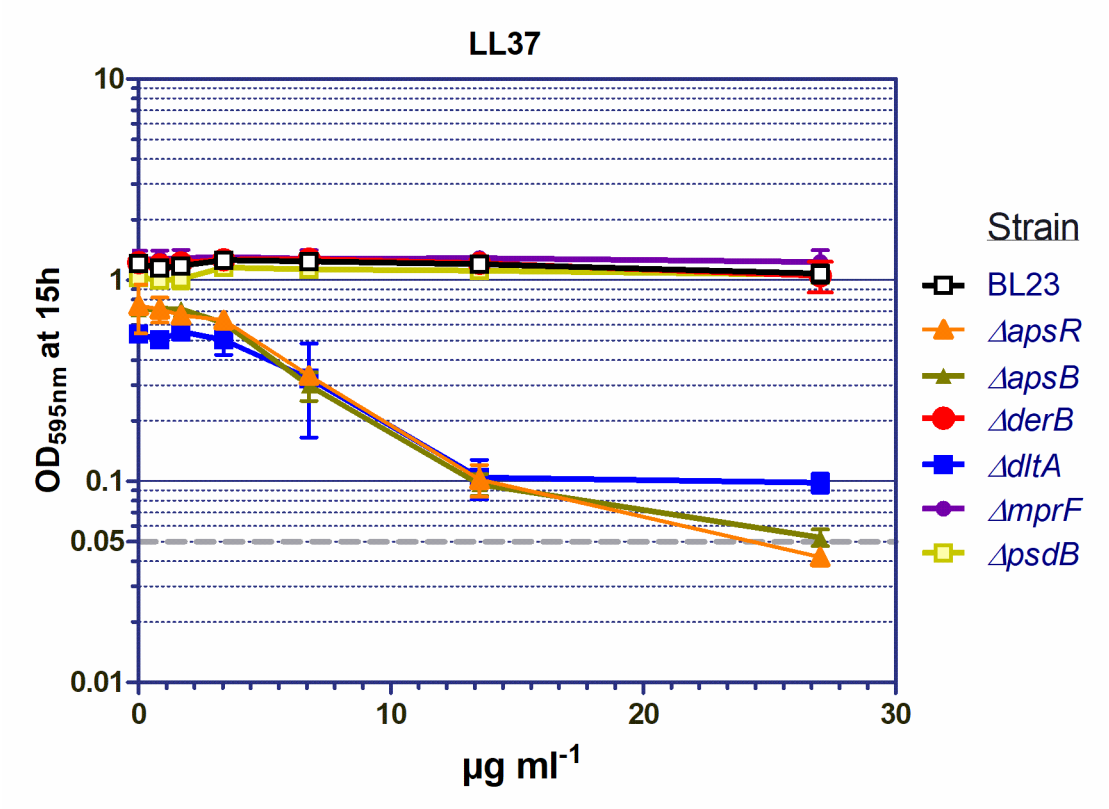

Supplemental figure 1: MIC of LL37 for *L. casei* BL23 and derivative strains. Strains were inoculated from overnight cultures to an OD_{595} of 0.05 (grey dashed line) in MRS with different serial dilutions of LL37. Final OD_{595} readings were taken after 15h incubation at 37°C (OD_{595} 15h). MIC was defined at the lowest antibiotic concentration where the final OD was at or below the starting OD. Mean and standard deviation are presented.

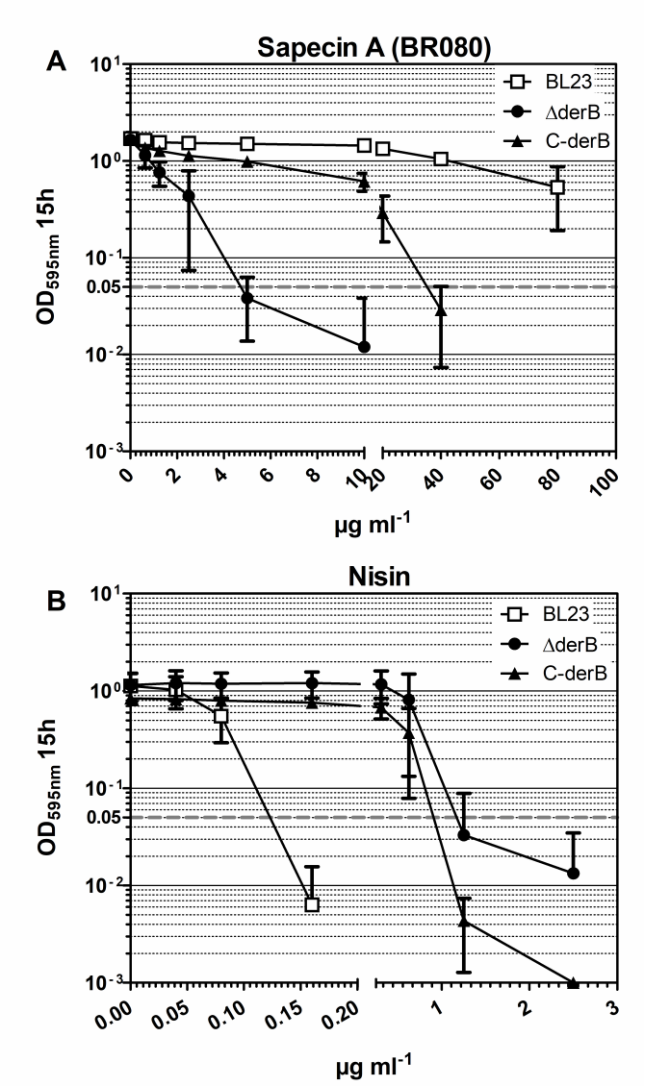

Supplemental figure 2: MIC of Sapecin A (BR080) (A) and Nisin (B) for C-*derB* (the *ΔderB* complemented strain). The *L. casei* BL23 and the *ΔderB* mutant strain are shown for comparison. Strains were inoculated to an OD_{595} of 0.05 (dashed line) in MRS with different concentrations of antibiotics. Final OD_{595} readings were taken after 15h incubation at 37°C (OD_{595} 15h). MIC was defined at the lowest antibiotic concentration where the final OD was at or below the starting OD. Mean and standard deviation of triplicates are presented. Different stock solutions of nisin (Sigma-Aldrich N5764: Nisin from *Lactococcus lactis* 2.5% (balance sodium chloride and denature milk solids)) and sapecin A (chemically synthetized by Covalab S.A.S., Villeurbanne, France for the experiments presented in Figure 2 and by Panatecs® Heilbronn, Germany for the experiments presented in Sup. Fig. 2) might account for the different MIC values observed for strain BL23 and *ΔderB* mutant on Figure 2 and Sup. Fig. 2. Notwithstanding, the overall relative sensitivities were very well reproduced.

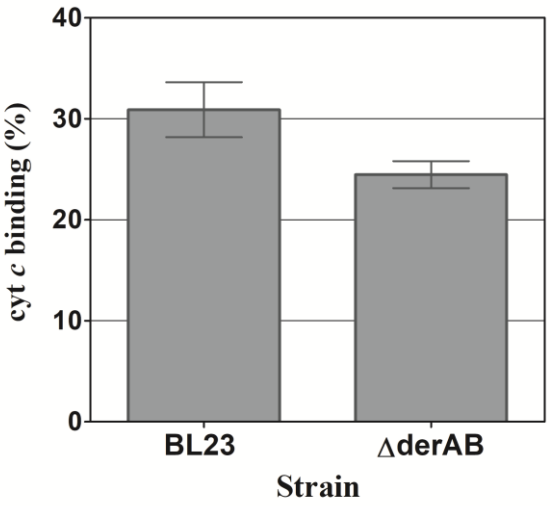

Supplemental figure 3: Cytochrome *c* (cyt *c*) binding in stationary phase. Binding is expressed as the percentage of cyt *c* bound to stationary-phase cells of strain BL23 and *ΔderB* after incubation with 150 µg ml^{-1} cyt *c* for 10 min at room temperature. Data represent the means and standard deviations from three independent experiments. Unpaired Student *t* test showed no significant differences between the strains.

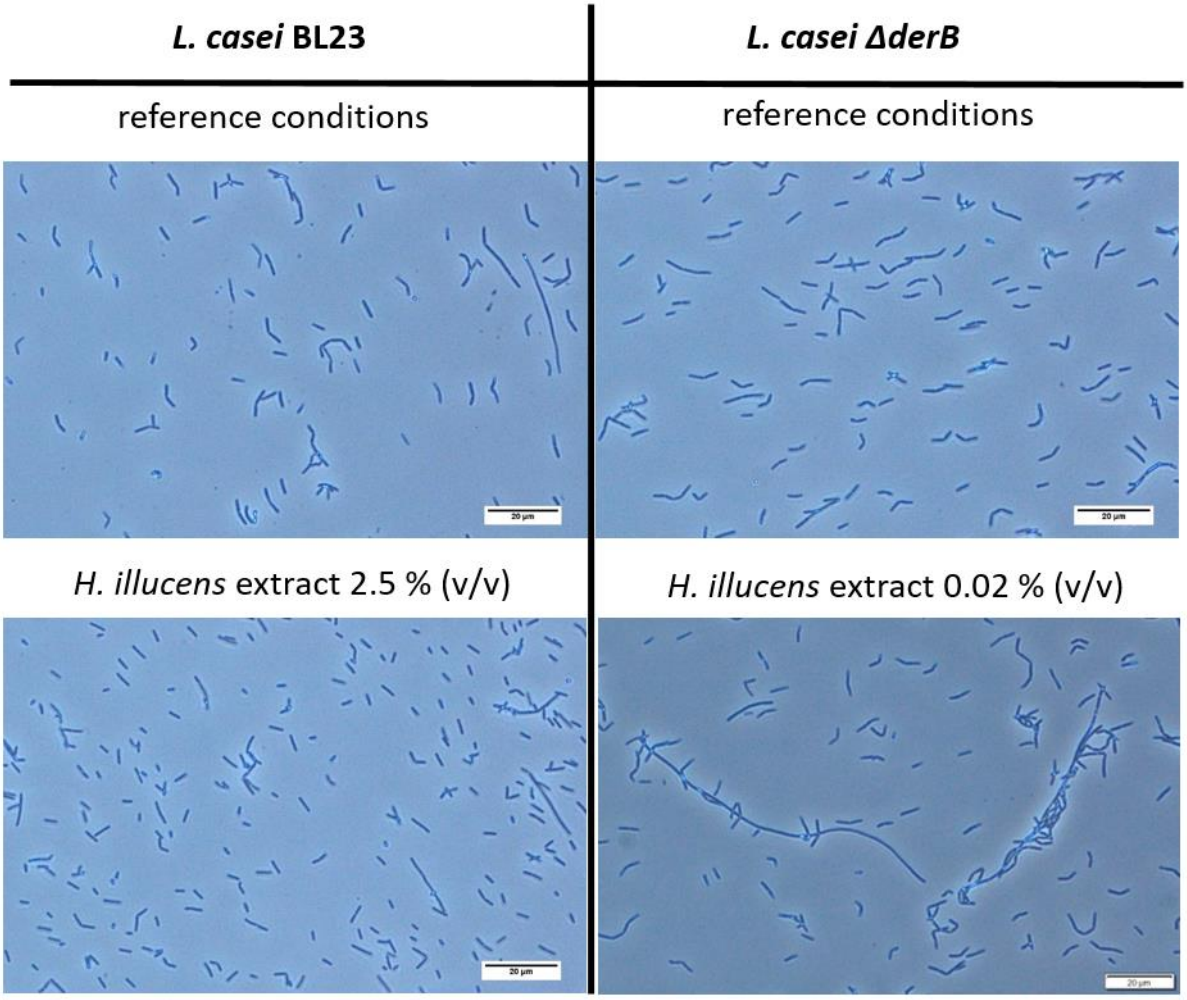

Supplemental figure 4: Microscopy of *L. casei* BL23 and derivative strain *ΔderB* after exposition to *H. illucens* extract. Stationary phase cell cultures of BL23 (left column) and *ΔderB* (right column) grown for 24 hours under reference conditions (top pictures) or in the presence *H. illucens* extract (bottom pictures) were photographed (phase contrast, 40x magnification). Due to the different sensitivities' phenotypes of wild type and mutant strain (See Fig. 2G in the main text), the pictures were made after exposition to a concentration of the extract of 2.5 % (v/v) for the wild type and 0.02 % (v/v) for the mutant. Scale bar 20 µm.

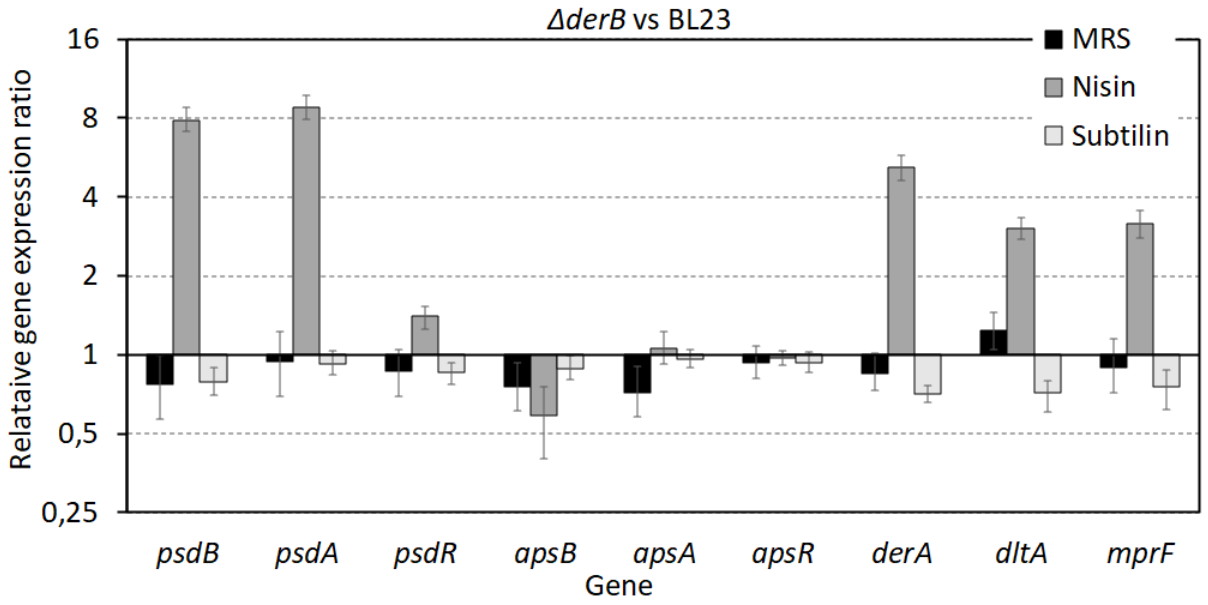

Supplemental figure 5: Expression of known nisin and subtilin resistance determinants in *ΔderB* mutant background. Transcript levels were determined by real-time RT-PCR in reference conditions, 10 min after addition of 22.5 ng ml^{-1} nisin and 10 min after addition of 1% subtilin. X-fold induction of known nisin and subtilin resistance genes in *ΔderB* strain were calculated relative to transcript levels in the parental strain *L. casei* BL23 under the same conditions. Data are shown as mean ± standard error of at least six replicates.

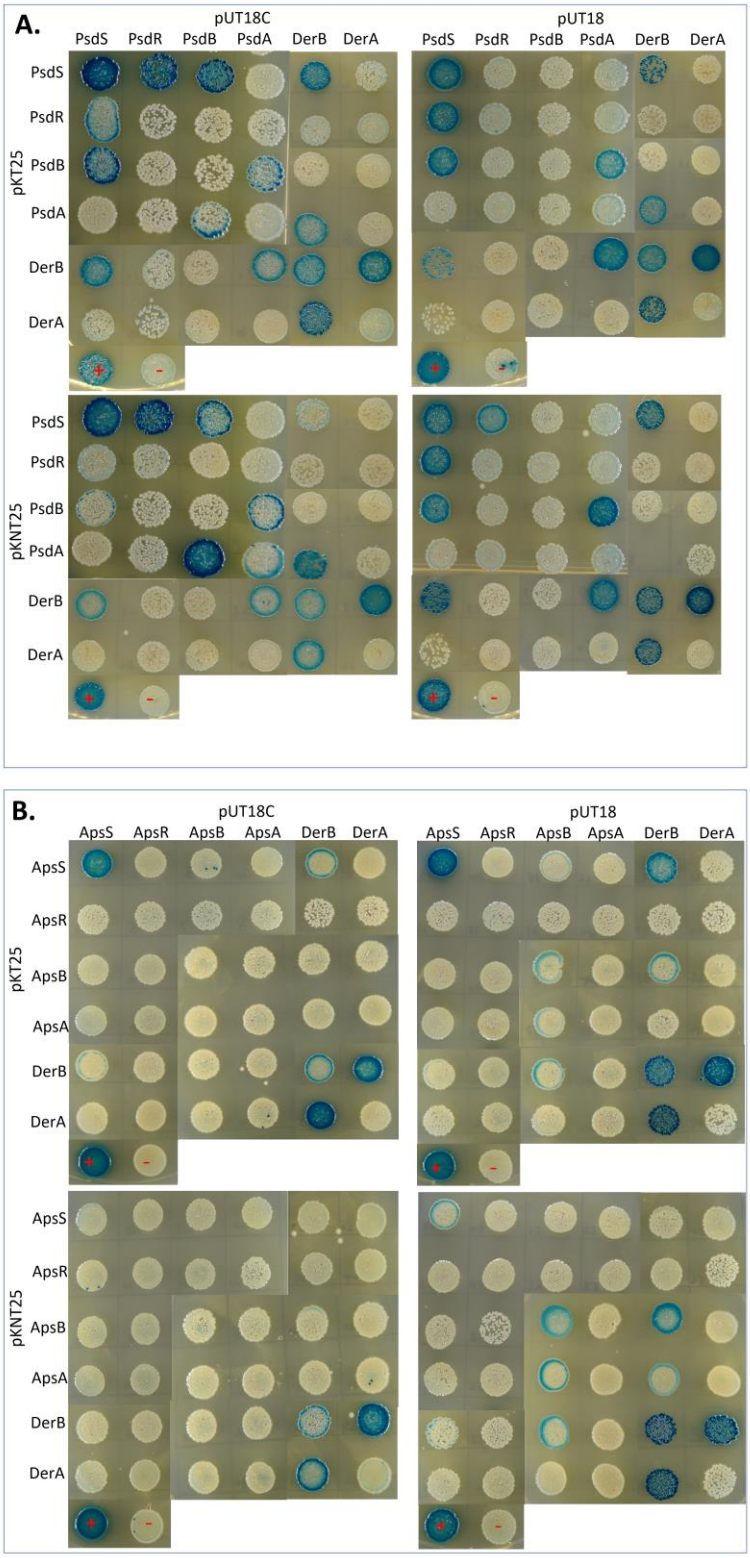

Supplemental figure 6: Complete data set for the bacterial two-hybrid analysis. The interactions of DerAB proteins with the PsdRSAB module proteins are shown in the four panels in **(A)** and the interactions of DerAB proteins with the ApsRSAB module proteins in the four panels in **(B)**.

C-terminal and N-terminal translational fusions of the T18 and T25 domains of CyaA of *B. pertussis* were created for each protein individually. The expression vectors are indicated in the *y* and *x* axis.

pKT25 and *pKNT25* both encode the T25 fragment (first 224 aminoacids of CyaA), they are low-copy number plasmids expressing kanamycin resistance. *pKT25* allows in-frame fusions at the C-terminal end of the T25 polypeptide (T25 - protein of interest); *pKNT25* allows in-frame fusions at the N-terminal end of T25 (protein of interest - T25).

pUT18 and *pUT18C* both encode the T18 fragment (amino acids 225 to 399 of CyaA), they are high copy number plasmids expressing ampicillin resistance. *pUT18* allows in-frame fusions at the N-terminal end of T18 (protein of interest - T18); *pUT18C* allows in-frame fusions at the C-terminal end of the T18 (T18 – protein of interest).

The plasmids *pKT25-zip* and *pUT18C-zip* served as positive controls for complementation (shown as "+") and vectors *pKT25* and *pUT18C* as negative controls (shown as "-").

Different hybrid fusions were tested in pairwise combinations in *E. coli* BTH101. The cells were spotted onto LB plates containing X-Gal (100 µg ml^{-1}), IPTG (1 mM), and antibiotics for selection. Pictures were taken after 48 h of incubation at 30 °C. The blue colonies indicate positive interaction results.

Sequence Identity matrix (BLAST)									
	BR081	BR087	BR088	BR089	BR091	plectasin	BR090	BR080	BR092
BR081	100,0								
BR087	44,0	100,0							
BR088	35,0	70,0	100,0						
BR089	28,0	48,0	44,0	100,0					
BR091	35,0	45,0	48,0	38,0	100,0				
plectasin	51,0	44,0	42,0	38,0	35,0	100,0			
BR090	n.a.	54,0	52,0	46,0	47,0	39,0	100,0		
BR080	38,0	75,0	90,0	43,0	40,0	46,0	57,0	100,0	
BR092	35,0	75,0	88,0	43,0	48,0	42,0	55,0	95,0	100,0

Supplemental figure 7: Sequence identity matrix of the defensins under study. Text color code indicates if both (bold green), one (bold black) or none (bold red) of the compared defensins are substrates of the DerAB transporter. Comparison between two defensins from the same group shown in Supplemental figure 7 are highlighted with background colors: group I- pink; group II- yellow; group III- blue. The identity values (indicated as a %) were obtained after sequence comparison of the defensins with Protein BLAST program (https://blast.ncbi.nlm.nih.gov/Blast.cgi). n.a. not available.